



# **Volcán Barú—Eruptive History and Volcano-Hazards Assessment**

By David R. Sherrod, James W. Vallance, Arkin Tapia Espinosa, and John P. McGeehin

Open-File Report 2007–1401

**U.S. Department of the Interior**  
**U.S. Geological Survey**

**U.S. Department of the Interior**  
DIRK KEMPTHORNE, Secretary

**U.S. Geological Survey**  
Mark D. Myers, Director

U.S. Geological Survey, Reston, Virginia 2008

For product and ordering information:  
World Wide Web: <http://www.usgs.gov/pubprod>  
Telephone: 1-888-ASK-USGS

For more information on the USGS—the Federal source for science about the Earth,  
its natural and living resources, natural hazards, and the environment:  
World Wide Web: <http://www.usgs.gov>  
Telephone: 1-888-ASK-USGS

Suggested citation:  
Sherrod, D.R., Vallance, J.W., Tapia Espinosa, A., and McGeehin, J.P., 2008, Volcan Baru—eruptive history  
and volcano-hazards assessment: U.S. Geological Survey Open-File Report 2007–1401, 33 p., 1 plate, scale  
1:100,000.

Available on World Wide Web at <http://pubs.usgs.gov/of/2007/1401>

Any use of trade, product, or firm names is for descriptive purposes only and does not imply  
endorsement by the U.S. Government.

Although this report is in the public domain, permission must be secured from the individual  
copyright owners to reproduce any copyrighted material contained within this report.

# Volcán Barú—Eruptive History and Volcano-Hazards

By David R. Sherrod<sup>1</sup>, James W. Vallance<sup>1</sup>, Arkin Tapia Espinosa<sup>2</sup>, and John P. McGeehin<sup>3</sup>

## Introduction

Volcán Barú is a potentially active volcano in western Panamá, about 35 km east of the Costa Rican border. The volcano has had four eruptive episodes during the past 1,600 years, including its most recent eruption about 400–500 years ago. Several other eruptions occurred in the prior 10,000 years. Given this history, Volcán Barú will erupt again, following some premonitory period of seismic activity and subtle ground deformation that may last for days or months. Future eruptions will likely be similar to past eruptions—explosive and dangerous to those living on the volcano’s flanks. Outlying towns and cities could endure several years of disruption in the wake of renewed volcanic activity. Thus, when Volcán Barú becomes restless, national, provincial, and local officials need to respond swiftly.

This report is divided into two parts. The first is an executive summary that describes, in general terms, the volcanic products of Volcán Barú and its volcano-hazard potential. That part is intended for those who desire a short

informed discussion of past geologic events and likely outcomes from future eruptions.

The second part delves more deeply into the scientific methods, data, and findings of our study. It includes the complete results of reconnaissance mapping and stratigraphic studies, radiocarbon dating, lahar-inundation modeling, and hazard-analysis maps. Existing data have been compiled and included to make this report as comprehensive as possible.

## Part 1. Summary of volcano hazards

Volcán Barú, Chiriquí Province, is situated south of the continental divide in the Cordillera de Talamanca of western Panamá (fig. 1). Its summit, 3,374 m altitude, towers about 2,000 m above populated valleys to the west and about 2,400 m above those to the east. More than 10,000 people live in areas immediately adjacent to the volcano, where the hazards from future eruptions are greatest. The heavily populated Pacific coastal plain, crossed by the Pan-American Highway, lies 30 km to the south.

Volcán Barú has been built by numerous eruptions dating back several hundred thousand years. The volcano is notable for its young, large andesitic to dacitic dome complex nested within a horseshoe-shaped amphitheater carved into the older part of the volcanic edifice (fig. 2). Eruptions of the past few thousand years have been from vents on the summit dome.

---

<sup>1</sup> U.S. Geological Survey, Vancouver, WA 98683, U.S.A.

<sup>2</sup> Department of Geosciences, University of Panamá, Panamá City, Republic of Panamá

<sup>3</sup> U.S. Geological Survey, Reston, VA 20192, U.S.A.

Their products have been distributed chiefly to the west and southwest. The amphitheater itself formed when a substantial part of the volcano slid away as a large debris avalanche, probably more than 50,000 years ago. Today the escarpment walls expose the volcano's older pyroclastic rocks and lava flows.

Little is known about the extent of damage inflicted by the most recent eruption of Volcán Barú, which may have occurred as recently as A.D. 1550. But it, like eruptions of the three previous eruptive episodes of the past 1,600 years, probably was prolonged over several years. Volcán Barú's eruptive episodes typically have included widespread tephra fallout, pyroclastic flows, and lahars. If such eruptions were to occur now, many people and costly infrastructure would be at risk.

## Volcanic Phenomena

Volcanoes pose a variety of geologic hazards, shown synoptically in figure 3. Many of the hazardous events depicted have occurred at Volcán Barú in the past and are likely to occur in the future. The eruption of molten rock, or **magma**, sparks most of these events. Others, such as landslides and some lahars, can occur without eruptive activity. The style of eruptive activity depends on the size and type of volcano, the composition of the magma, and interactions between magma and ground water. **Composite volcanoes**, like Volcán Barú, are long lived, episodically active, and characterized by a variety of eruptive products

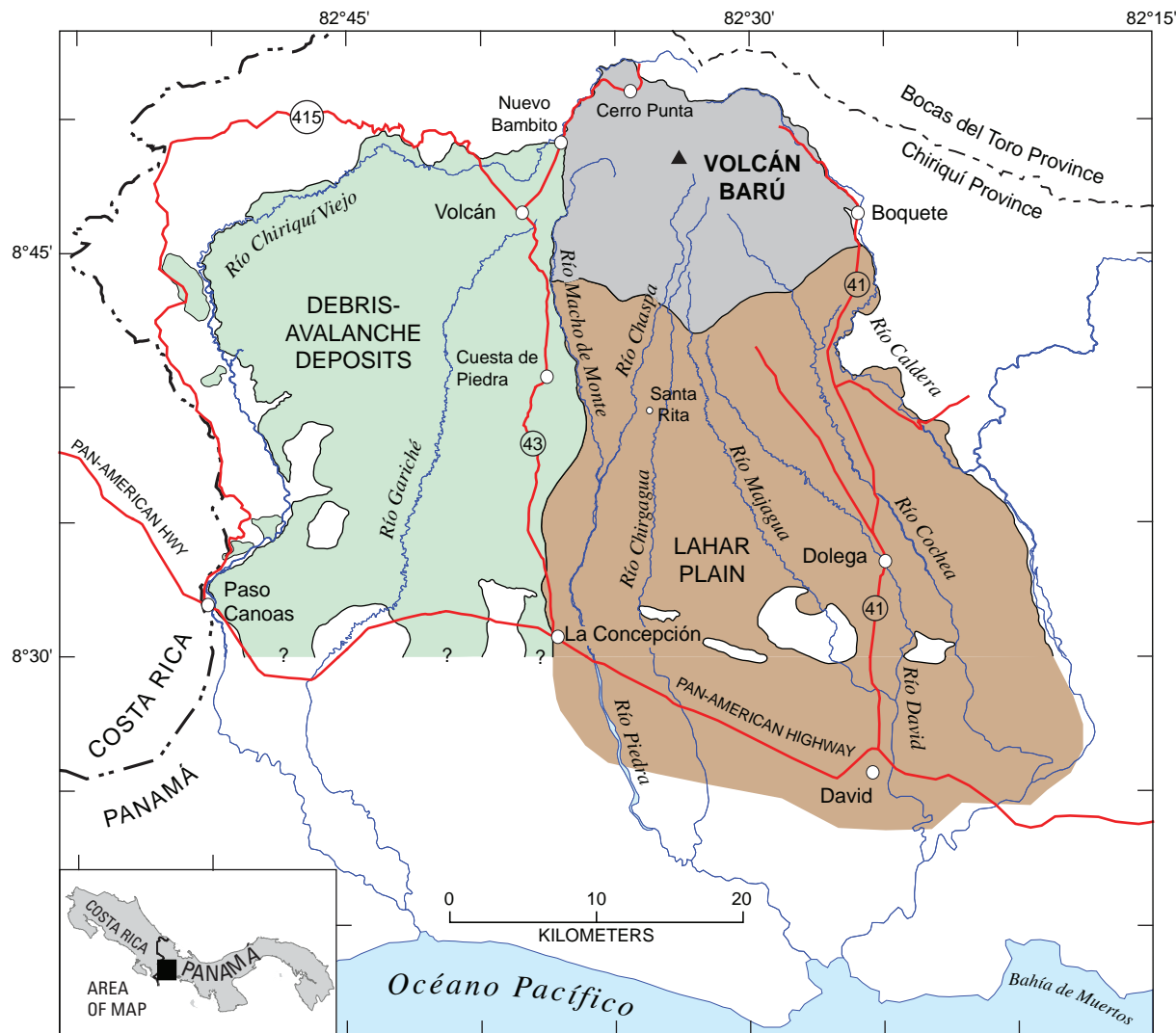


**Figure 1.** Location of Volcán Barú, Chiriquí Province, western Panamá. Province boundary in northeast approximates continental divide. Shown queried is southern limit of debris avalanche deposits that formed following a prehistoric collapse of Barú. Brown shading, lahar plain on south and southeast flanks. Base generalized from Instituto Geográfico Nacional, David, 1:250,000 scale, edition 2.

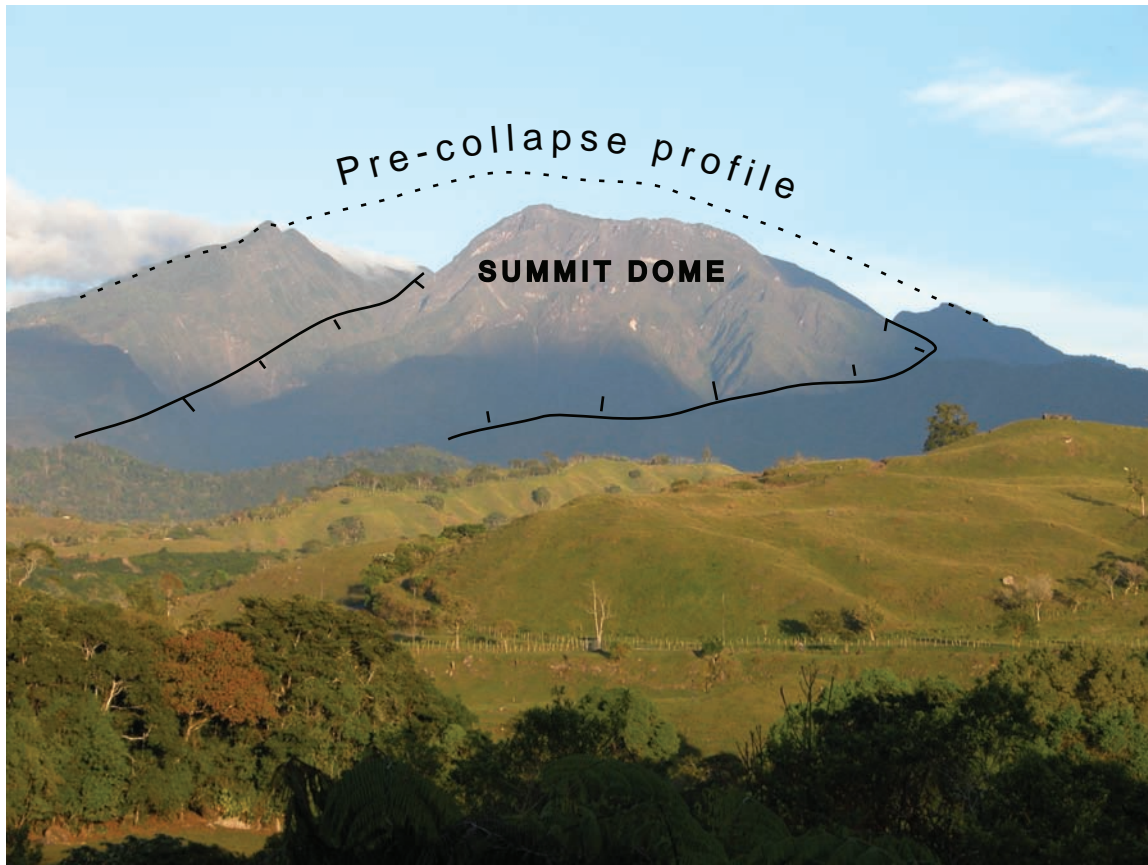


**Figure 2.** View east to Volcán Barú, from 15 km distance. Foreground is hummocky terrain underlain by debris-avalanche deposits from Barú. Hachured lines approximate the headwall of ancient debris avalanche.

across a range of chemical composition. At Volcán Barú the volcanic rocks are chiefly andesite and basaltic andesite but include sparse dacite.

## Tephra

### General description

As magma nears the surface of a volcano it releases dissolved gases. The rapidly expanding gas shreds the solidifying magma. If the resulting fragments exit the conduit at great velocity, they are thrust high into the atmosphere. Volcanologists use the term **tephra** for such fragments, which range in size from microscopic ash to meter-sized blocks. As tephra falls from eruption clouds (fig. 3), it commonly is deposited in broad lobate sheets downwind from the volcano. A large deposit can cover areas tens to hundreds of kilometers from the source, its thickness and particle size decreasing away from the vent. The largest tephra fragments fall to the ground within a few kilometers of the vent.

Tephra fallout seldom threatens life except within a few kilometers of a vent, where it may accumulate to thicknesses in excess of 1 m. The impact of large fragments close to the vent can cause death or severe injury. Large projectiles, if hot, may start fires where falling onto combustible material.

Perhaps the greatest threat from tephra fallout, and the cause of most injuries and fatalities, results when thick or wet accumulations collapse the roofs of buildings. Fine tephra suspended in the air can irritate eyes and lungs, especially among the elderly and infants.

Tephra falls reduce visibility. Tephra clouds can create darkness lasting tens of minutes or more, even on sunny days. The ash can contaminate surface water, plug storm- and sanitary-sewer systems, and clog irrigation canals. Even thin accumulations may ruin crops. Tephra can short-circuit electric transformers and break power lines, especially if it is wet, sticky, and heavy. Fine ash is drawn into engines, clogging filters or increasing wear. Ash ingested by jet engines abrades the turbines and other internal parts and melts in the hot engine, causing malfunction and power loss. Even small, dilute tephra clouds at great distance from a volcano can damage jet aircraft that fly into them.

### At Volcán Barú

Prehistoric eruptions of Volcán Barú have repeatedly spread tephra blankets more than 100 km downwind and deposited thicknesses of 10 to 20 cm at distances 10 to 15 km downwind (fig. 4). A tephra fall of such magnitude can darken skies, cause panic among some residents, and ultimately cause



roofs of some houses to collapse. Tephra clouds of the size that have occurred at Volcán Barú in the past might rise as high as 10 km or more above the volcano. Many of the ash clouds will be composed of fine ash.

## Pyroclastic flow and surge

### General description

When the mixture of hot gases and volcanic rock particles produced by an explosive eruption is denser than air, it behaves like a fluid, staying close to the ground and flowing downslope as a **pyroclastic flow** (fig. 3). If the mixture contains a large proportion of particles, then its density will tend to funnel it into topographically low areas, like quebradas and valleys. Voluminous pyroclastic flows or sequences of such flows, especially on the slopes of the cone, may fill valleys and sweep across low divides between adjacent drainages.

**Pyroclastic surges**, a related phenomenon, are dilute mixtures of hot ash and gas commonly generated from pyroclastic flows. Pyroclastic surges can separate from the pyroclastic flow and move onto higher areas adjacent to or beyond the margins of pyroclastic flows.

Pyroclastic flows and surges move at speeds of 50 to 150 km per hour, easily overtaking anyone on foot. Temperatures in pyroclastic flows and surges commonly are several hundred degrees Celsius or more. Pyroclastic flows destroy structures and kill all living things in their paths. Though somewhat less destructive, pyroclastic surges can affect larger areas and be lethal. Pyroclastic surges often cause severe burns, trauma to the lungs, or suffocation.

### At Volcán Barú

Pyroclastic flows have been common during eruptions of Volcán Barú. The type most common at Barú, **block-and-ash flows**, has originated by the collapse of hot lava from the steep slopes of the summit lava dome (fig. 5). Block-and-ash flows of the past 1,600 years have descended westward from the summit area toward and through the present-day town of Volcán (plate 1). Indeed, Volcán is built on block-and-ash flow deposits many meters thick. These block-and-ash flows have been limited to an area within 15 km from their source at the summit dome.

### Lava flows

If magma degasses sufficiently before reaching the Earth's surface, it may erupt

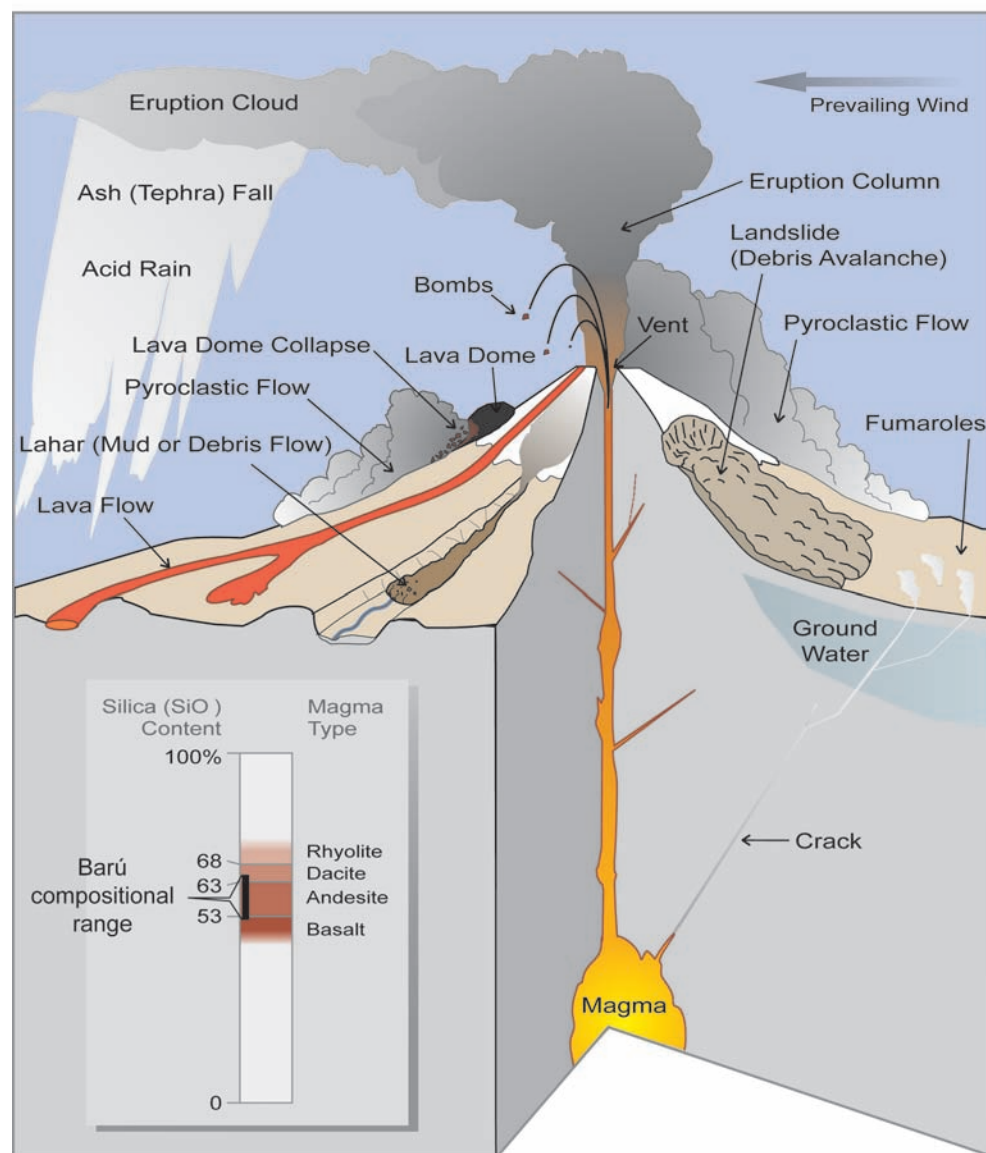


**Figure 3.** Sketch showing hazardous events associated with a volcano like Barú. Some events, such as lahars and landslides (debris avalanches), can occur even when the volcano is not erupting. Inset box shows classification of magma types on basis of silica content; range for analyses at Volcán Barú from figure 7 and appendix 1. Sketch from Myers and others (2002).

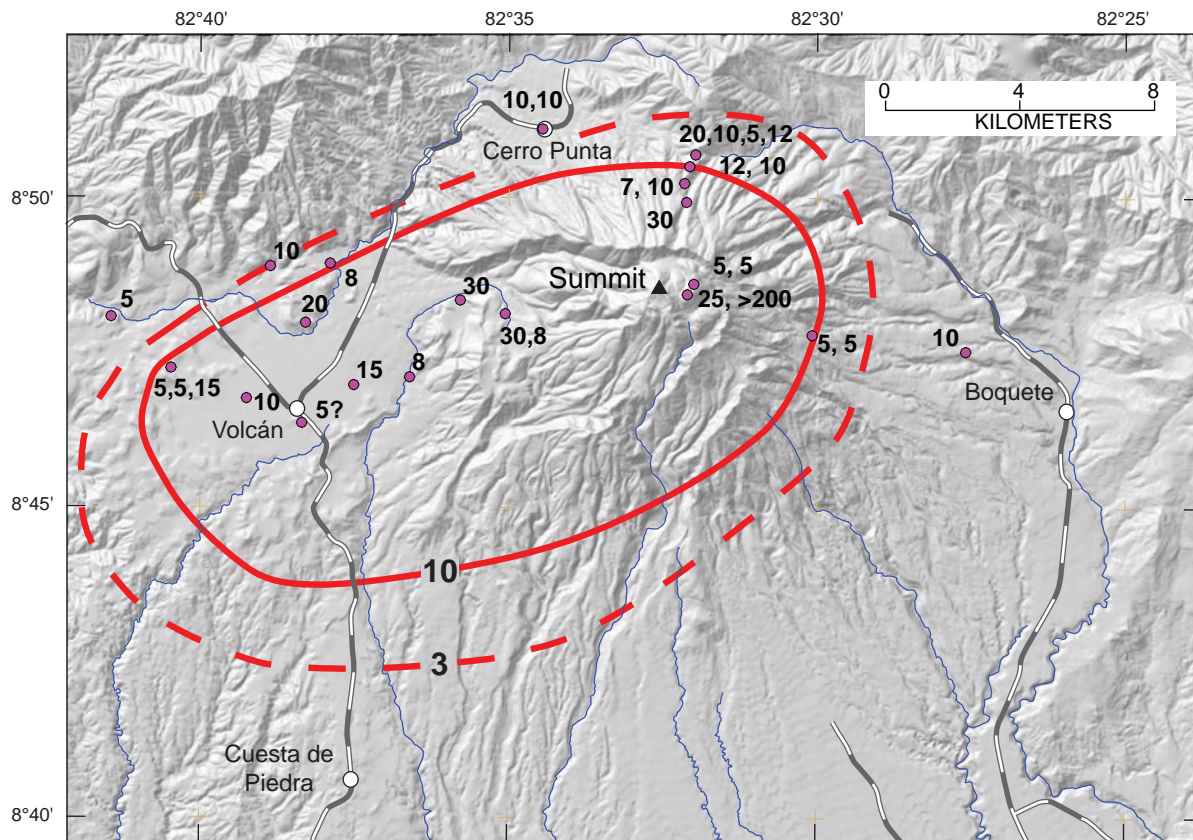


**Figure 4.** Characteristic thickness, in centimeters, of fallout tephra around volcano. Sample locations show one or more thicknesses measured from stratigraphic sections. Isothickness lines indicate 3- and 10-cm accumulations of youngest tephra fall.

passively to form **lava flows**. Lava flows that have formed at Volcán Barú are extremely viscous, blocky, and slow moving. Such lava flows commonly advance downslope as boulder-mantled streams of rock tens of meters thick. They move at rates of meters to a few tens of meters per day. Lava flows can be extremely destructive but they typically are not life threatening, because people can walk fast enough to escape. Lava flows on the steep upper slopes of Barú, however, present some local hazards because they are unstable; they could avalanche from their snouts to form hot block-and-ash flows from which there is little chance of escape.

Stubby lava flows of the past few thousand years have built Barú's summit dome. They have moved westward, though never more than about 2 km from source (fig. 6). In future eruptions, however, the flow directions may differ. Although the ancient avalanche scarp has directed these lava flows westward, the moat between the scarp and the summit is now nearly full. If the moat were overtopped, future lava flows could descend the steep eastern slopes of the volcano toward the town of Boquete.

With few exceptions, the area of greatest lava-flow hazards at Volcán Barú—outward to 5 km—is uninhabited (fig. 6). This area likely would be closed to access during future eruptions owing to the overall high hazard there from pyroclastic flows, tephra fallout, and volcanic gases.

## Volcanic gases

All magmas release gases during and between eruptions. Volcanic gases include steam, carbon dioxide, sulfur dioxide, and trace amounts of several other gases. The gases dissipate rapidly downwind from the vent but are potentially toxic within a few kilometers of a vent. Gases can injure eyes and lungs. In closed depressions, gases that are denser than air, like carbon dioxide, can accumulate and cause suffocation. The greatest hazards from volcanic gases preceding or during the next eruption at Volcán Barú will be within 1–2 km of the summit dome or in the moat to the east (fig. 6). These uninhabited areas likely would be closed to access during future eruptions, owing to the overall high hazard there from several volcanic phenomena.

## Debris avalanches and landslides

### General description

The steep upper slopes of a volcano may be notably unstable during eruptions. Their failure can create a rapidly moving **landslide** called a **debris avalanche**. Magma intrusion and volcanogenic earthquakes can cause slope instability and



deep-seated failure like the one that occurred in 1980 at Mount St. Helens, U.S.A. Slope failures may also be triggered by tectonic earthquakes larger than about magnitude 5, torrential rains, or steam explosions. These failures are commonly orders of magnitude smaller in volume than those triggered by magmatic intrusion.

Debris avalanches can attain speeds in excess of 150 km per hour. Debris avalanches with volumes less than a million cubic meters typically travel only a few kilometers from their source. In contrast, large-volume debris avalanches can travel tens of kilometers beyond a volcano. Debris avalanches

destroy everything in their paths. The resulting deposits range from 10 m to more than 100 m thick on valley floors.

## At Volcán Barú

Many thousands of years ago Volcán Barú was gutted by a huge debris avalanche, a relatively rare event. Consequently, the hazard of huge-avalanche recurrence has been diminished substantially. Instead, much smaller debris avalanches are more likely and would possibly occur by partial slumping or collapse of the summit dome. But even their likelihood is relatively small. The resulting deposits would be restricted to an area outward from the mouth of the amphitheater toward Nuevo Bambito and downslope toward Volcán.

## Lahars

### General description

**Lahars**, also called volcanic mudflows and debris flows, are masses of mud, rock, and water that look and behave much like flowing concrete. They occur when water mobilizes large volumes of loose mud, rock, and volcanic debris. They also form when landslides and avalanches contain or incorporate enough water to become fluid, a fairly common occurrence.

Lahars, like floods, follow river valleys and then spread out to inundate floodplains and low-lying areas. They can travel many tens of kilometers downvalley at speeds of tens of kilometers per hour. Lahars destroy or damage everything in their paths through burial or impact. They leave deposits of muddy sand and gravel several meters or more in thickness. Lahars are particularly hazardous because they travel farther from a volcano than any other hazardous phenomenon except tephra, and they affect valley floors where human settlement is usually greatest.

In some instances, lahars clog stream channels or block tributaries so that water collects behind the blockage. The impounded water can spill over the blockage, quickly cut a channel, and catastrophically drain out, generating floods and yet more lahars that move down the valley. Breaching of such blockages may occur within hours or months after impoundment.

Like floods, lahars range greatly in size. The amount of available water and loose volcanic debris determines lahar size. Eruptions can dump millions of cubic meters of sediment into channels that, when mixed with water during subsequent rains, causes lahars. The smallest lahars recur most frequently (perhaps every few years), whereas the largest recur on the order of centuries to millennia.

## At Volcán Barú

At Volcán Barú, many streams are incised in steep-sided canyons, so the damage from lahars trapped within them will be limited to the canyon itself. The largest lahars may reach

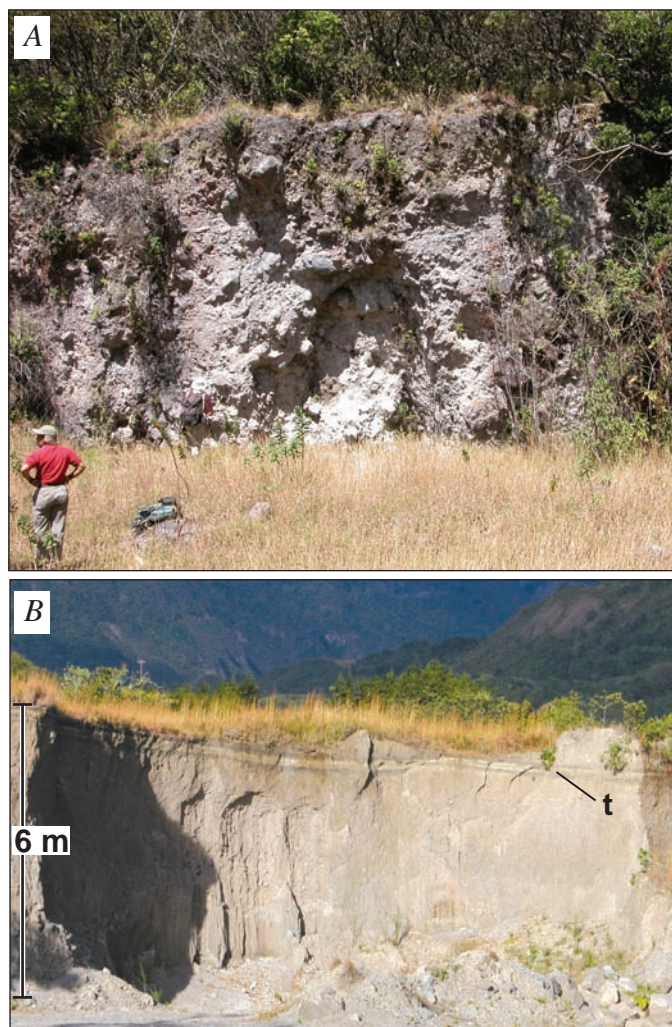


**Figure 5.** Pyroclastic-flow deposits, Volcán Barú. *A*, Coarse deposit near foot of summit dome, 4.3 km west of summit. Exposure is about 10 m high. Large blocks are dense hornblende andesite and dacite. *B*, Finer-grained pyroclastic-flow deposit in quarry 10 km west-southwest of summit, near Volcán town. Characteristic pale reddish gray color from oxidation of iron-bearing minerals during cooling. Large dense blocks are lacking here owing to distance of transport, and deposit at this distance is slightly pumiceous. Thin light-colored band near top (t) is tephra-fall deposit, which lies between dark-gray paleosols. Sequence is capped by another thin pyroclastic-flow deposit.



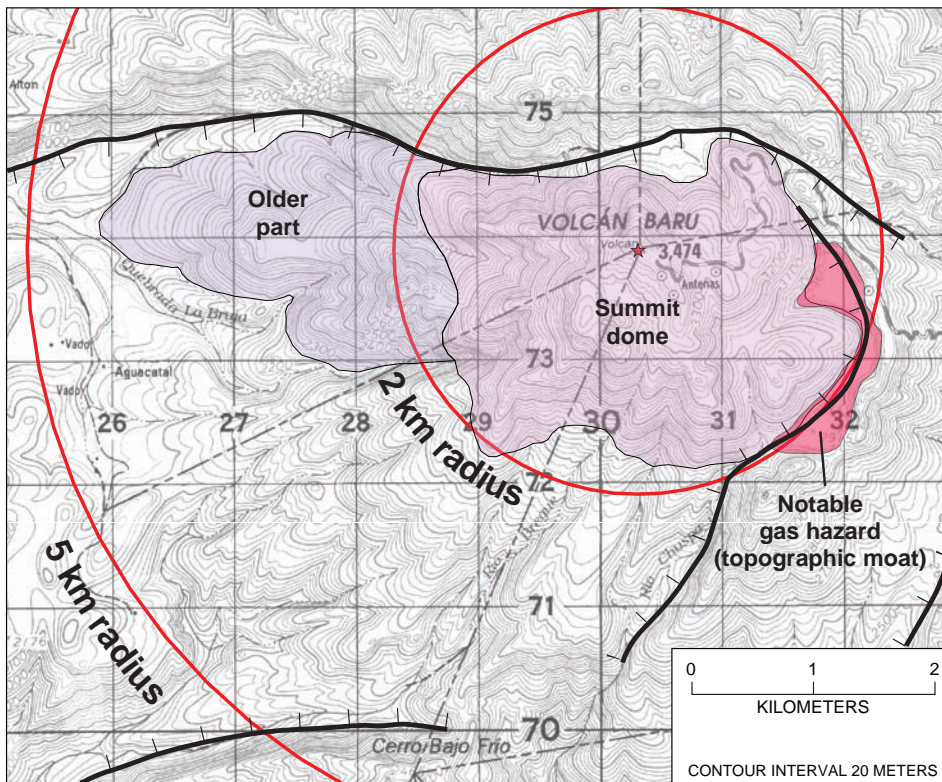


**Figure 6.** Details of summit area showing 2- and 5-km radius from vent and extent of recent lava dome, which lies entirely within the 2-km zone. Topographic depression, or moat, could be overtopped by future dome growth, allowing lava flows to travel down the east flank. The moat also corresponds to notable gas hazard. Hachured lines show base of headwall of ancient debris avalanche.

to midslope altitudes on the plain from La Concepción to the Río Caldera, where the canyons broaden and lose topographic relief (plate 1). In this area the largest lahars can spread more widely.

In contrast, the Volcán area, although close to the volcano, lies upon a broad plain. Lahars from the mouth of the amphitheater would spread across this plain and then be funneled in the canyons of the Río Chiriquí Viejo and Río Macho de Monte (plate 1). Exceptionally large lahars may reach to the Río Gariché and then be funneled downvalley until they deplete their mass.

Landslides and lahars may cause problems for years after the original eruptions end. Once lahars have filled stream channels with sediment, the streams begin to erode new paths. The new stream channels can be highly unstable and shift rapidly as sediment is eroded and moved farther downvalley.

## Monitoring and warnings

Future eruptions at Volcán Barú would be preceded by premonitory activity such as shallow earthquakes, deformation of the edifice, increased gas emissions, or steam explosions. Rising magma will cause shallow earthquakes beneath the edifice for days to weeks prior to an eruption. Deformation of the volcanic edifice in areas surrounding the site of a future vent commonly precedes eruptions. Changes in the composition, temperature, or volume of volcanic gases emanating from the area of past fumaroles in the moat near

the summit might also indicate a buildup to an eruption. Steam explosions are common as magma nears the surface, where it interacts with ground water. When any of these events are recognized, emergency-management agencies need to increase the level of monitoring and inform people potentially at risk.

A well-maintained seismic network comprising at least three stations remains the best single investment for volcano monitoring, but other monitoring can be useful once unrest begins. As of October 2007, Volcán Barú is monitored by nine seismic stations, a network built and managed by the University of Panama's Institute of Geosciences. An additional monitoring scheme that could be added is a network of continuously operating Global Positioning Satellite (GPS) receivers. A worthwhile real-time GPS monitoring network also requires three or four instruments, both for redundancy (in the event that a single station fails) and to verify that signals from one station are not simply a localized nonvolcanic response. Measurements of gas flux and composition and heat flux can indicate changes related to magma movement.

The hazard zones described here (plate 1) are defined broadly. Particular sites that might be affected within each zone cannot be specified in advance. Once precursory activity or an eruption begins, scientists can better define areas likely to be affected.

When an episode of volcanic unrest continues or increases in intensity, an eruption may be imminent. Local authorities will need to respond by informing residents of the risk or by moving them to safe areas away from the volcano. Single dwellings and small settlements are scattered on the flanks of the volcano. In the event of an episode of continuing or

intensifying unrest, people living in these sparsely populated areas need to be informed about volcano hazards and be prepared to evacuate. Residents of nearby communities and towns downslope of the volcano need to be informed of volcanic risks specific to their areas and, in some cases, may need to be evacuated. Planning ahead for these contingencies is prudent because once an emergency begins, public resources can often be overwhelmed.

## Part 2. Geologic history and its bearing on the volcano-hazards assessment of Volcán Barú

### Setting and composition

Volcán Barú lies near the southern end of the Central American volcanic arc. It is situated inboard of the Nazca Plate, which is subducting obliquely beneath Panamá. The regional tectonic setting is made more complex by the subduction of the Caribbean Plate behind the arc as well.

The volcanic rocks of Volcán Barú range in composition from 52 to 65 weight percent  $\text{SiO}_2$  (fig. 7). They contain moderate  $\text{Na}_2\text{O}$  and  $\text{K}_2\text{O}$  and are classified as basaltic

andesite, andesite, and low-silica dacite (Le Bas and Streckeisen, 1991). Their fractionated rare-earth-element geochemistry (high La:Yb ratio, for example), high Sr content, and no Eu anomaly (de Boer and others, 1988) are characteristics that might be expected of erupted products at the ends of volcanic arcs where the subduction-related magmatic component is diminished commensurate with diminished rate of subduction.

Reports of seismicity at Volcán Barú are vague and incomplete, especially those possibly related to volcano-tectonic activity. Notable swarms occurred in September 1930, June–August 1963, November 1985, and May 2006 (Eduardo Camacho, Univ. Panamá, written commun., 2007; Randall White, USGS, written commun., 2007). According to de Boer and others (1988, p. 278), “seismic activity (harmonic tremors) in 1963 below the Barú volcanic complex indicated rising magmas” [parentheses in original]. Skepticism, however, is warranted here: the characterization of the 1963 swarm as tremor or related to magma movement is without basis.

### Volcanic edifice

The edifice of Volcán Barú, a large cone covering 280  $\text{km}^2$ , was built by numerous overlapping pyroclastic flows, lahars, and lava flows (fig. 8). The ancestral summit may have risen to an altitude of 3,800–4,000 m prior to its excavation by the west-flank debris avalanche (appendix 2). The pre-avalanche

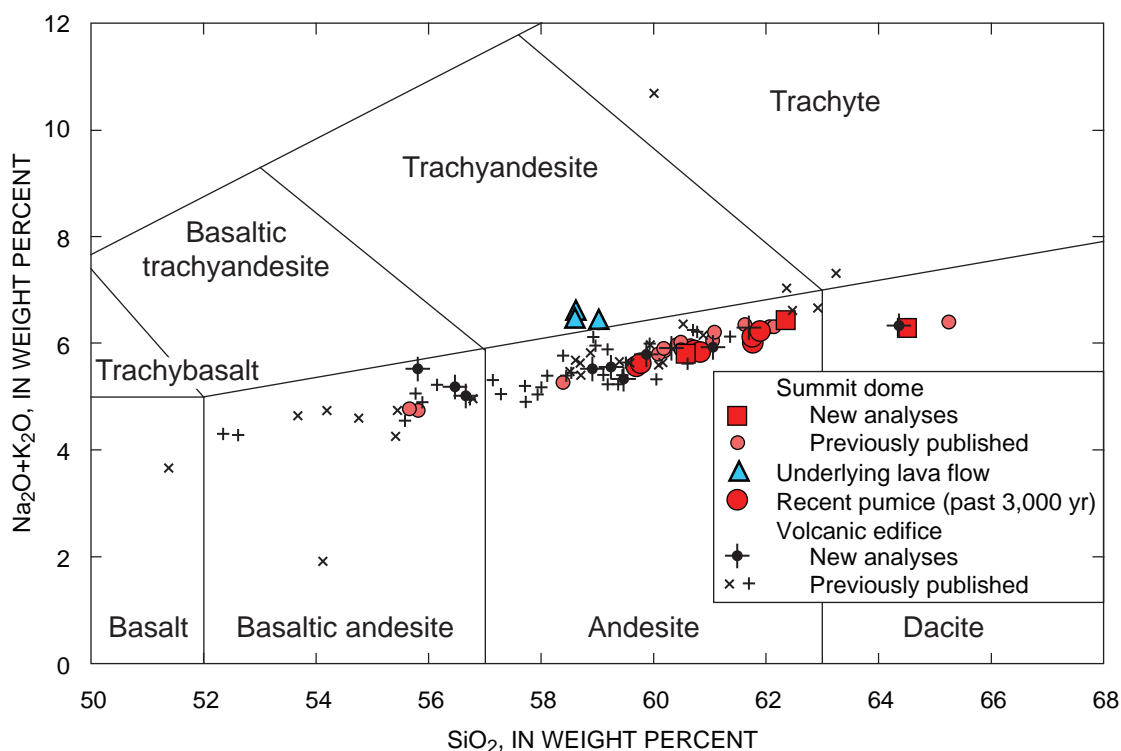
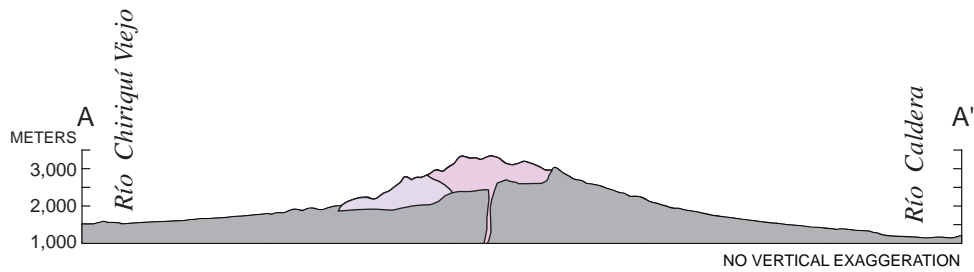
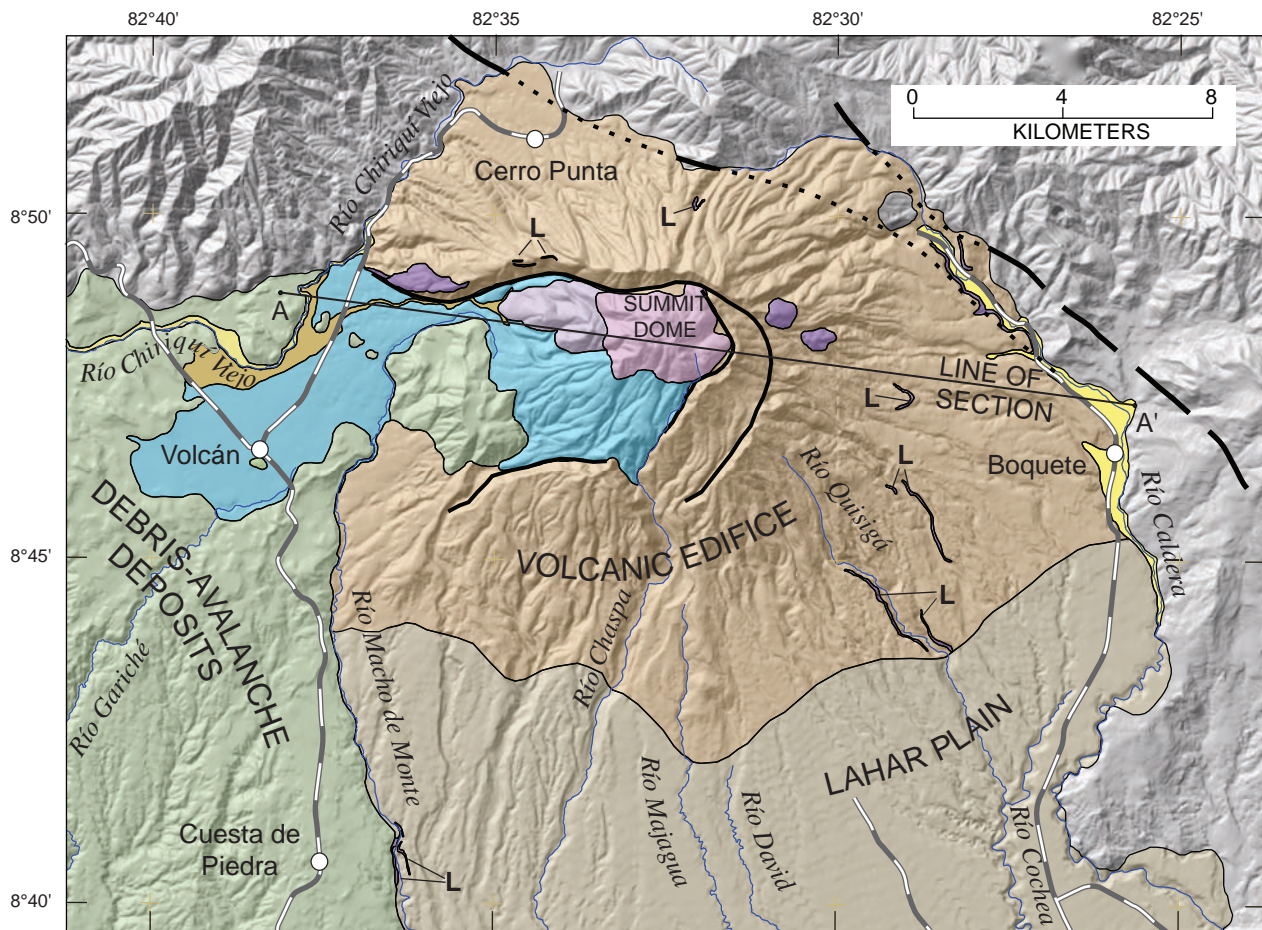


**Figure 7.** Silica vs. total alkalis variation diagram. Data from appendix 1, including 22 new analyses and results published previously by Restrepo (1987) and Rausch (2007). Analyses normalized to 100 percent  $\text{SiO}_2$ , volatile free. Classification grid from Le Bas and Streckeisen (1991).





EXPLANATION	
	Alluvium (Holocene)
Rocks and deposits near Volcán and in amphitheater	
	Lahars of Nuevo Bambito (Holocene)
	Young block-and-ash deposits (Holocene)
	Summit lava dome (Holocene)
	Older part (Pleistocene?)
Southwest of volcano	
	Debris-avalanche deposits (Pleistocene)
	Lahar plain
	Lahar deposits (Holocene and Pleistocene)
Volcanic edifice	
	Older lava domes and lava flows (Pleistocene)— Labeled "L" where canyon-wall exposures are too narrow to show readily on map
	Pyroclastic-flow and lahar deposits, sparse lava flows (Pleistocene)
	Fault, dotted where concealed
	Amphitheater escarpment headwall

**Figure 8.** Reconnaissance geologic map of Volcán Barú, from this study. Hillslope shaded-relief base map from topographic maps of Instituto Geográfico Nacional, scanned by Titan Averstar Inc. and modeled by U.S. Geological Survey.



edifice had a volume of 250–350 km<sup>3</sup>, an estimate whose wide range results from the uncertain depth to the base of the volcano (appendix 2). A few lava domes dot the flanks, cover less than 2 percent of the area, and likely are a small part of the volcano, volumetrically. Topographic relief is about 2,400 m along an east-west cross section at the latitude of Boquete, measured from the floor of the Río Caldera to the volcano's summit (fig. 8). Relief on the west side is slightly less, about 2,000 m. The edifice slopes, excluding the walls of the amphitheater, are in the range 10–30 percent (5.4–16.5°).

Lava flow thickness typically is 10–20 m, although some flows are as thick as 60 m. They are found chiefly within 11 km of the summit. An exception at greater distance is the basaltic andesite of the Río Macho de Monte (55.8 percent SiO<sub>2</sub>, appendix 1, sample S07-VB81B), a lava flow exposed at the hydroelectric plant east of Cuesta de Piedra, 16 km from the summit.

By some reports the volcano built a lava-flow edifice early in its history (for example, Terry, 1956). Our preliminary reconnaissance leaves uncertain the extent of lava flows within the edifice. On a previous map, lava flows are shown covering more than 50 percent of the edifice area (Universidad Tecnológica de Panamá, 1992). In contrast, lava flows form fewer than 20 percent of the beds exposed in a large

landslide scar as high as 400 m along the amphitheater walls, only 3.7 km north-northeast of the volcano's center (fig. 9). Elsewhere the lava flows thicken downslope, and their relative proportion may increase greatly outward on the volcano's flanks. An improved estimate of lava-flow abundance is a worthy future endeavor, since it may have a bearing on the volcano's tendency to erupt explosively or passively.

The oldest strata of Volcán Barú lie buried by subsequently erupted deposits, and none of the exposed older rocks have been dated. The few lava flows we have sampled possess normal-polarity thermal remanent magnetization and likely are younger than 0.78 Ma (mega-annums, or millions of years ago). A K–Ar whole-rock age from lava near Horqueta (5 km northwest of Boquete) yielded an age of 0.46±0.15 Ma (IRHE, 1985), likely the basis for a suggestion that volcanism began about 0.5 Ma (Universidad Tecnológica de Panamá, 1992). Volcán Barú is younger than Volcán Tisingal<sup>1</sup>, a similar but more deeply eroded composite volcano that lies adjacent to Barú on the west. Tisingal is extinct, inasmuch as

<sup>1</sup>Also referred to as *Cerro Colorado* or *Cerro Pelón* in the Earth sciences literature. Tisingal is used most commonly. The name *Cerro Colorado* is best retained for a porphyry copper deposit 80 km southeast.

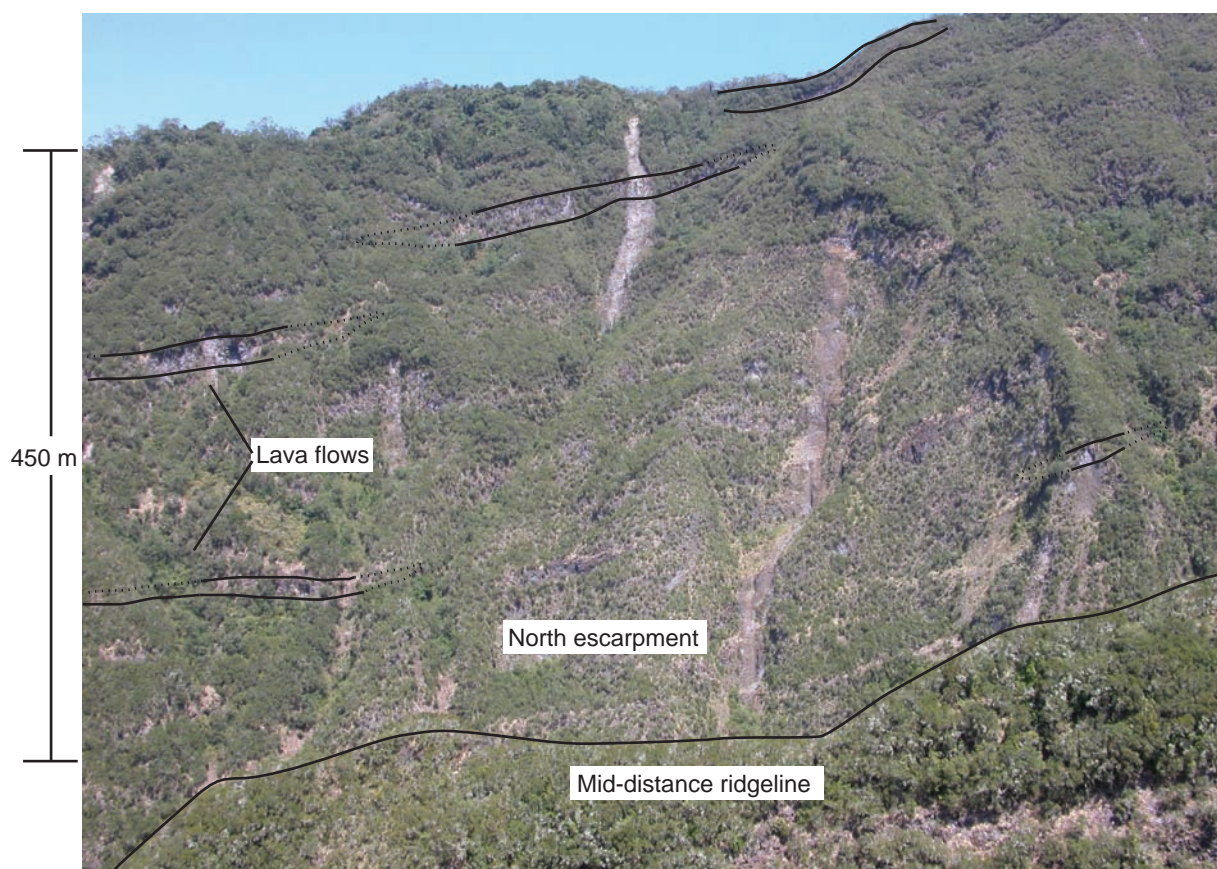


**Figure 9.** Photograph of north escarpment showing stratigraphic section comprising sparse interspersed lava flows (labeled) and thick pyroclastic flow deposits, lahar deposits, and thin tephra fall deposits (all unlabeled areas). View north-northeast from 2,400-m altitude on westside summit trail.

its radiometric ages are in the range 1.6–0.9 Ma (Universidad Tecnológica de Panamá, 1992) and no younger volcanic activity is known from it.

## Debris-avalanche deposits

The deposits of a large debris avalanche cover a swath 20 km wide that extends 30 km to the Pan-American Highway and beyond, perhaps reaching the Pacific Ocean (fig. 1). The extent and source of the debris-avalanche deposit originating at Volcán Barú was recognized previously on the basis of a large area of hummocky topography southwest of the volcano and a horseshoe-shaped amphitheater breached to the west (Siebert and others, 2006).

The avalanche deposits encompass about 25–30 km<sup>3</sup>, the largest example yet documented in Central America (Siebert and others, 2004, 2006; appendix 2). By way of comparison, the extent is nearly ten times larger than the notorious debris avalanche that occurred in 1980 at Mount St. Helens, U.S.A.

Agewise, little is known directly of the debris-avalanche deposits. They are older than about 8,740±90 <sup>14</sup>C yr B.P. (9,540 cal B.P.), which is the age of organic-rich silt beneath a terrace where the Río Chiriquí Viejo incised the margin of a large alluvial fan near Paso Canoas, a fan that itself probably formed in a short time after the emplacement of the avalanche deposits as the Río Chiriquí Viejo adjusted to landscape changes in its upslope reach (Hugh Cowan, New Zealand Earthquake Commission, written commun., 2007). A tree found in a deposit beneath the debris-avalanche deposit proved too old to date by radiocarbon (older than about 40,000–50,000 <sup>14</sup>C yr B.P.) (written commun., 2007, Tom Gardner, Trinity University; and Don Fisher and Kristin Morell, Pennsylvania State University), but conceivably a paleosol or unconformity separates the sample-bearing deposit from the avalanche deposit (Tom Gardner). In that case the older age is not a closely limiting maximum age of the avalanche.

Obtaining a maximum limiting age for the avalanche event may have been the reason for an earlier attempt to date a lava flow in the amphitheater wall southeast of Bambito. The resulting K–Ar age, 0.27±0.23 Ma (IRHE, 1985), has too large an analytical error to provide additional insight.

The eastern limit of the headwall amphitheater has subparallel escarpments (fig. 8), which may indicate more than one episode of flank failure (Siebert and others, 2006). The dual escarpments may also be interpreted as the boundaries of nested blocks that slid only slightly before stopping during a single collapse event, although subparallel escarpments are uncommon at other volcanoes that hosted large flank failures (L. Siebert, written commun., 2007). We treat the collapse and avalanche as a single event, for simplicity. Convincing evidence for multiple episodes would come from paleosols within the debris-avalanche deposits, which are little studied.

The hummocky terrain of the debris-avalanche deposits hosts many closed topographic depressions, some with lakes, especially in the area within 20 km of the volcano's summit. The occurrence of these depressions, surrounded by low

hills littered with blocks of lava, understandably led to an interpretation that numerous volcanic craters formed during small eruptive events across a broad field (for example, Stewart, 1978), although an insightful earlier interpretation suggested that faulting or eruption may have breached Volcán Barú and led to the formation of the deposits (Terry, 1956, p. 10–11). The lesson of the 1980 eruption at Mount St. Helens illuminated the process of catastrophic debris avalanches and led to the recognition of numerous such events worldwide, including the Panamanian examples at Barú and adjacent Volcán Tisingal (Siebert and others, 2006).

## Lahar plain

The south and southeastern volcanic flanks grade into a vast, slightly dissected volcanoclastic fan (“outwash plain” of Terry, 1956) built by lahars and alluvium from Volcán Barú (fig. 1). The fan has slopes less than 4 percent (1.5–2.0°). Lithologically it grades seaward from mostly lahars and pyroclastic-flow deposits near the volcanic edifice to a downslope assortment of lahars and alluvial deposits such as conglomerate and pebbly sandstone.

In its midslope reach the lahar plain is underlain by volcanoclastic strata more than 60–80 m thick, judging from the exposures along streams such as the Río Cochea upslope of Dolega or the Río Chaspa near Santa Rita. Along the eastern margin of the plain, the Río Caldera supplies some nonvolcanic material from adjacent older bedrock, but the preponderance of material must have been derived from Volcán Barú. The volume of volcanic material is difficult to estimate accurately, owing to uncertainty in its thickness and the manner in which it thins southward toward the ocean. North of lat 8°30' it covers 630 km<sup>2</sup> and likely encompasses a volume in excess of 60 km<sup>3</sup>. Farther south it may contain another 30 km<sup>3</sup>, but the distribution, thickness, and extent of interbedded nonvolcanoclastic deposits are poorly known.

## Summit dome

A lava dome and related pyroclastic-flow deposits and fallout tephra partly fill the eastern reach of Volcán Barú's debris-avalanche amphitheater (figs. 2 and 8). Probably all of the volcano's Holocene eruptive activity—that of the past 11,500 years—has originated from the area of the recent dome.

The summit dome is hornblende-bearing andesite and dacite lava (60–64 percent SiO<sub>2</sub>; fig. 7). Interlayered with the lava are pyroclastic-flow deposits of similar composition. Pyroclastic-flow and -fall deposits also form a steep flanking fan within the crater, on the dome's southwest side. An older, sparsely porphyritic pyroxene andesite lava (58–59 percent SiO<sub>2</sub>; fig. 7) underlies the summit dome (fig. 8). This older lava is probably a thick lava flow that originated from a vent now buried by the summit dome. It may be a slide block of nearly intact lava related to the collapse of the ancient cone, as shown on a previous geologic map (Universidad Tecnológica



de Panamá, 1992); however, it lacks the tilt-block morphology, seen in other nearby blocks, that results as a large block chatters apart during its transport. This sparsely porphyritic lava remains undated; it may have been emplaced soon after the amphitheater formed and be much older than the overlying summit dome.

The older, sparsely porphyritic andesite lava flow and the summit dome, stacked one above the other, form steep relief of 1,500 m on their west side, measured from the volcano summit to the floor of the amphitheater. This relief adds notably to the volcano hazards of renewed dome growth, as discussed later.

A few small topographic depressions lie along the east side of the summit dome where it impinges on the east crater wall (fig. 6). The largest contained a tepid sulfur spring in the past (Terry, 1956, p. 11). We have no information on current fumaroles or springs.

## Fallout tephra

Pumiceous lapilli and ash are found as fallout deposits 1–10 cm thick at distances ranging from 4 to 6 km on the volcano's north, east, and south flanks (fig. 4). Similar deposits are preserved at greater distance, as far as 20 km to the southwest, along the direction of the prevailing winds. A similar distribution was reported by Stewart (1978). The skewing of equal-thickness lines toward the west-southwest results from prevailing winds predominantly from the northeast or east-northeast.

Substantially thicker deposits occur at the summit and southwest within the amphitheater. A deposit of coarse pumiceous blocks greater than 2 m thick is exposed in a pit at the 3,300-m-altitude saddle on the road to the summit, and the deposit extends an unknown depth below the pit floor. At the Aguacatal site, 4.6 km west of the summit, a roadcut exposes more than 10 m of coarse fallout and pyroclastic flow deposits, perhaps the aggregate of several closely spaced eruptions that occurred prior to about 950 calibrated yr B.P., the age of charcoal (S07-VB93) in the paleosol above these deposits. These greater thicknesses are limited to areas near the dome and within the amphitheater.

## Pyroclastic-flow deposits

The summit dome at Volcán Barú has shed block-and-ash flows westward and onto the volcanoclastic fan that underlies Volcán town (fig. 8). These deposits are thicker than 6 m where exposed in quarries. They contain slightly pumiceous to dense blocks of hornblende-bearing andesite or dacite in an ashy matrix. Charcoal is found in a few (for example, sample RC-6E,  $855 \pm 35$   $^{14}\text{C}$  yr B.P.). Fine-grained ash forms surficial deposits in the terrain adjacent to the volcanoclastic fan, likely the result of pyroclastic surges or ash clouds billowing up and outward beyond the extent of the main pyroclastic flows.

The Volcán volcanoclastic fan encompasses 22 km<sup>2</sup> beyond the amphitheater. The volume of the pyroclastic-flow deposits is estimated to be 2.2 km<sup>3</sup>. Individual flows likely were in

the range 10–100×10<sup>6</sup> m<sup>3</sup>, an estimate derived from the areal extent of inferred narrow elongate lobes whose emplacement would create the topographic features and the length and breadth of the entire fan.

## Dating the volcano's recent eruptive history

We deciphered Volcán Barú's eruptive history of the past few thousand years from its volcanic deposits, their ages, and intervening soil horizons (paleosols) preserved at various sites around the volcano. Radiocarbon ages of several deposits add a numerical time scale to the sequence of events.

Used judiciously, paleosols provide a rich record of eruptive episodes. Paleosols at similar stratigraphic positions at numerous sites suggest periods of volcanic quiescence. Overlying volcanic deposits mark renewed volcanism. An age from charcoal or wood at the top of a widespread paleosol indicates the age of the overlying volcanic deposit and the onset of a new volcanic episode. Thus, interpreted together, the volcanic deposits, interbedded paleosols, and ages define eruptive episodes not readily apparent from the radiocarbon ages alone. Intensity of soil development (thickness, depth of oxidation, extent of clay development) suggests the length of the quiescence, although other factors such as climate, altitude, and geography also affect soil-forming processes and may complicate the interpretation.

Eleven radiocarbon ages pertinent to eruptive events at Volcán Barú were obtained from wood and charcoal samples collected during field work in 2007 (table 1, fig. 10). Most ages are from charcoal at or near the top of paleosols mantled by tephra-fall deposits. Three additional ages useful for interpreting volcanic events resulted from a coring of Laguna Volcán, as part of a paleobotanical investigation (table 2; Behling, 2000). An age from an archaeological study is closely tied stratigraphically to the highest tephra fall near the Barriles cultural site (Linares and others, 1975). Other ages arising from that study are discussed briefly in appendix 3. New radiocarbon ages unrelated to volcanic events are listed in appendix 4. The locations and stratigraphic settings of all new samples are described in appendix 5.

The carbon-14 content of the atmosphere fluctuates irregularly with time, so that ages in radiocarbon years ( $^{14}\text{C}$  yr B.P., before present) may not correspond closely to calendar years, creating a variable time scale. For comparing different ages or discussing periodicity and rate, we present our results as calibrated ages, using correlations developed between tree-ring calendar ages and radiocarbon ages (Stuiver and Reimer, 1993). Calibrations are made using the CALIB program, version 5.0.1 (<http://calib.qub.ac.uk>), in conjunction with a recent decadal atmospheric  $^{14}\text{C}$  database (Reimer and others, 2004). Calibrated and radiocarbon ages are reported relative to A.D. 1950 (the "present"), the point at which atmospheric testing of hydrogen bombs loaded the atmosphere with



artificially produced  $^{14}\text{C}$  and rendered radiocarbon dating nearly useless for younger materials.

A fence diagram (fig. 11) shows the relation between volcanic deposits and paleosols at five sites on the volcano's summit and west flank. The variable deposition or preservation of specific deposits across the volcano, represented in the fence diagram by pinching of units, shows the difficulty of correlation without several dated samples.

The youngest ages tied to volcanic events range from about 370 to 3,030  $^{14}\text{C}$  yr B.P. and date tephra-fall deposits in the summit area and fall and pyroclastic-flow deposits on the southwestern volcanic plain near Volcán (tables 1, 2). Older ages, ranging from about 8,300 to 13,300  $^{14}\text{C}$  yr B.P., were obtained from the volcano's east flank upslope of Boquete and north of the volcano at Respingo saddle (table 1).

Several of the ages overlap within their analytical uncertainty, but the combination of ages, the distribution of paleosols, and the correlation of units among several sites indicate at least four major eruptive episodes in the past 1,600 years (fig. 12, table 3). Deposit sequences (for example, table 3) suggest that these episodes involved prolonged dome growth, explosive eruptions, and the spalling of numerous block-and-ash flows.

The four youngest age determinations mark the onset of a volcanic episode that began sometime between about 400 and 550 calibrated years B.P. (between A.D. 1550 and 1400). Two samples are from the base of tephra falls, the youngest fall deposits seen at each site, and one is from fine ash overlying the youngest tephra. Their assignment to a single eruptive event is based on this stratigraphic observation and their overlapping ages (fig. 12). The fourth sample, whose age dates the root of a tree buried by subsequent lake deposits, presumably marks the time when the Río Chiriquí Viejo was dammed or diverted by pyroclastic flows encroaching north of Volcán town.

The next oldest eruptive episode is undated. Its existence is known from extensive exposures at a quarry near Volcán and the Aguacatal site, where the occurrence of two paleosols and interbedded tephra above an older, dated pyroclastic-flow sequence establish the sequence of events (fig. 13, table 3).

The products of the third oldest eruptive episode lie beneath the aforementioned two paleosols. A charcoal sample (RC-6E) collected from within a pyroclastic-flow deposit at the Volcán quarry yielded a calibrated age between 690 and 900 cal yr B.P. The sample from the Aguacatal site within the large amphitheater of Volcán Barú is 800–950 cal yr B.P.

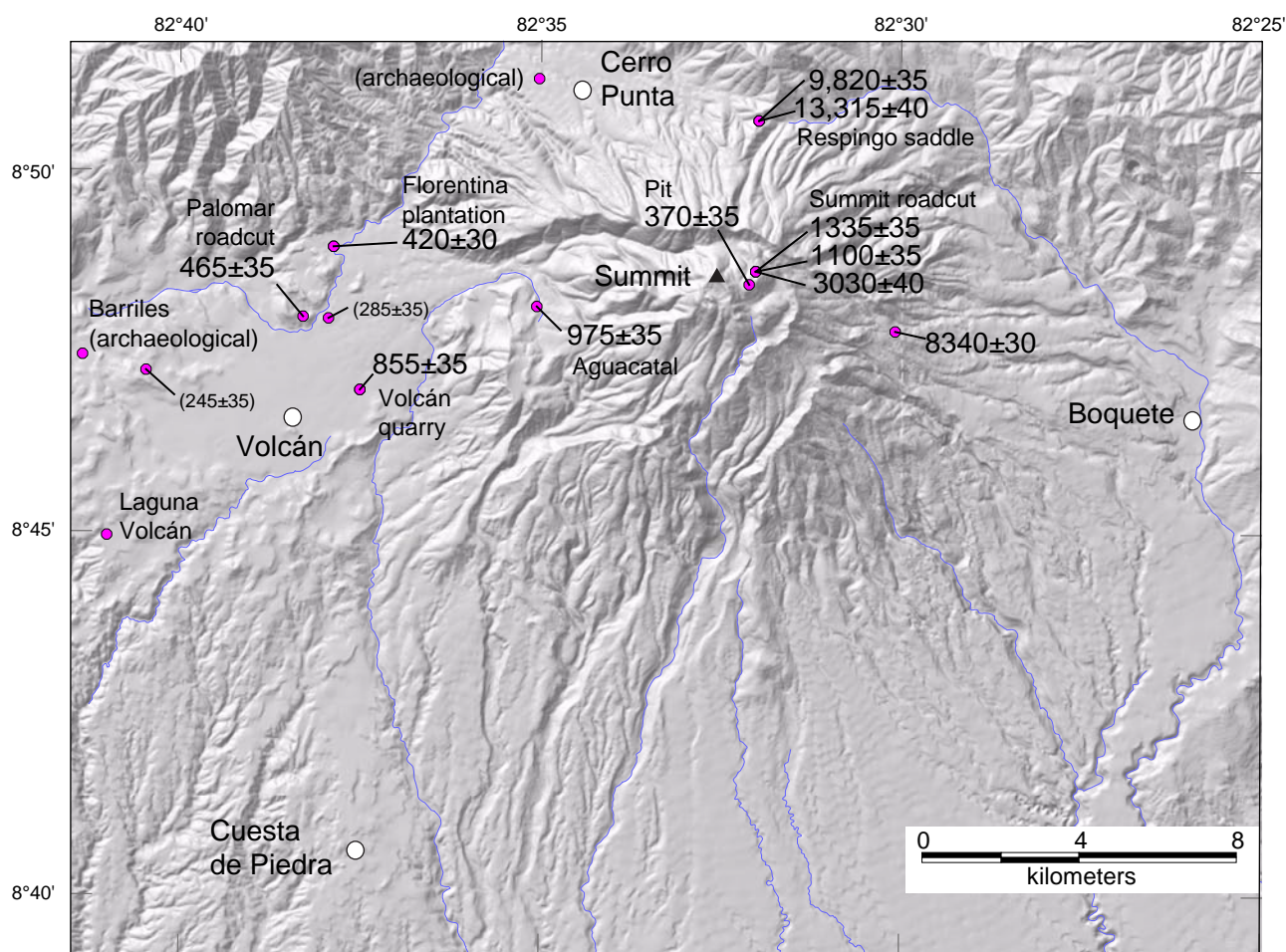


**Figure 10.** Radiocarbon age localities. Parenthetical ages not related to volcanic events, as discussed in text. Site names correspond to figure 12. Ages in radiocarbon years before present ( $^{14}\text{C}$  yr B.P.). Laguna Volcán is site dated by Behling (2000). Ages from archaeological sites were reported by Linares and others (1975), who showed generalized locations (their fig. 3).

**Table 1.** New radiocarbon and calibrated ages for samples that date volcanic events, Volcán Barú, Republic of Panamá.

[Samples prepared at U.S. Geological Survey Radiocarbon Lab, Reston, Va. Ages determined on July 2, 2007, by mass spectrometric methods at the Center for Accelerator Mass Spectrometry, Lawrence Livermore National Laboratory, Livermore, Calif. Four samples analyzed for per mil variation of  $^{13}\text{C}$  from expected value; other samples have presumed value of -25. Ages calibrated using CALIB radiocarbon calibration program, version 5.0.1 (Stuiver and Reimer, 1993) in conjunction with decadal atmospheric  $^{14}\text{C}$  database (Reimer and others, 2004). Probabilities show percentage of the 95 percent confidence age intervals, rounded to nearest 1 percent. Column for calendar ages is in years A.D. unless stated otherwise.]

Lab No.	Sample No.	Material dated	$\delta^{13}\text{C}$ , per mil	$^{14}\text{C}$ age, yr B.P.	$\pm (1\sigma)$	Calibrated age B.P.			A.D. Calendar age	
						Young	Old	Probability, (% of $2\sigma$ )	Young	Old
WW6166	RC-61-1	charcoal	-25	370	35	316	407	0.45	1634	1543
						421	504	0.55	1529	1446
WW6189	RC-2-3	wood	-23.08	420	30	333	351	0.07	1617	1599
						435	523	0.93	1515	1427
WW6162	S07-VB88-1	charcoal	-25	465	35	474	544	1.00	1476	1406
WW6165	RC-6E	charcoal	-25	855	35	688	801	0.85	1262	1149
						811	828	0.03	1139	1122
						862	903	0.12	1088	1047
WW6171	S07-VB93	charcoal	-25	975	35	794	938	0.98	1156	1012
						944	953	0.02	1006	997
WW6168	RC-62-0	charcoal	-23.52	1,345	30	1182	1206	0.10	768	744
						1236	1309	0.90	714	641
WW6169	RC-62-1	charcoal	-25	1,100	35	933	1067	1.00	1017	883
WW6167	RC-62-2	charcoal	-25	3,030	40	3,081	3,092	0.02	1131 B.C.	1142 B.C.
						3,110	3,126	0.02	1160 B.C.	1176 B.C.
						3,140	3,356	0.96	1190 B.C.	1406 B.C.
WW6161	S07-VB56A	charcoal	-24.79	8,340	30	9,285	9,456	1.00		
WW6164	S07-VB98-2	charcoal	-24.72	9,825	30	11,200	11,261	1.00		
WW6163	S07-VB98-1	charcoal	-25	13,315	40	15,450	16,179	1.00		

**Table 2. Radiocarbon and calibrated ages for previously published samples thought to date volcanic events, Volcán Barú, Republic of Panamá.**

[All are bulk soil samples. Ages calibrated to calendar years using Calib 5.0.1 software (Stuiver and Reimer, 1993). Probabilities show percentage of the 95 percent confidence, rounded to nearest 1 percent. Column for calendar ages is in years A.D.]

Lab No.	Depth, cm	Material dated	<sup>14</sup> C age, yr B.P.	± (1σ)	Calibrated age B.P.		Calendar age	
					Young	Old	Young	Old
I-7236 <sup>1</sup>	10–20	Bulk soil charcoal	740	150	500	962	A.D. 1450	A.D. 988
Beta 95496 <sup>2</sup>	42	Bulk soil charcoal	500	60	335	349	1615	1601
					440	442	1510	1508
					454	572	1496	1378
					579	652	1371	1298
Beta 95497 <sup>2</sup>	76	Bulk soil charcoal	1,020	60	793	1,056	1157	894
Beta 95498 <sup>2</sup>	88	Bulk soil charcoal	1,790	50	1,569	1,825	381	125
					1,852	1,858	98	92

<sup>1</sup> Data from Linares and others (1975).

<sup>2</sup> Data from Behling (2000).

The Aguacatal sample overlies pumiceous tephra fallout and underlies pyroclastic-surge deposits, and two more paleosols (table 3). These paleosols indicate two major eruptive hiatuses (or nondeposition at this site) in the time after 800 cal yr B.P., not including the quiescence of the modern period. A limiting age from a paleosol beneath the basal fall deposit at Laguna Volcán is 800–1050 cal yr B.P.

Not assigned to any of the three eruptive episodes just discussed, though certainly belonging to one of them, is an age from the youngest tephra-fall deposit found at Barriles, an archaeological site 6 km west-northwest of Volcán (Linares and others, 1975). The age has large analytical error (740±150 <sup>14</sup>C yr B.P.), which leads to the notably large range for its calibrated age (fig. 12). The Barriles tephra deposit likely belongs to the youngest eruptive episode, judging from the 20-cm thickness of fallout deposits at the Palomar plantation roadcut and 22-cm thickness in the Laguna Volcán coring. The laguna site is only 4 km southeast of the Barriles habitation, and both sites are at similar radial distance from the volcano's summit.

The fourth eruptive episode, which began sometime around 1,180–1,310 cal B.P., has corresponding deposits dated from the volcano's summit area and Cerro Punta (fig. 12). Units at the Aguacatal site that underlie three paleosols probably correlate with this episode of volcanism. Deposits include block-and-ash-flow deposits, pyroclastic-surge fallout, and a pumiceous tephra (table 3).

## Other data bearing on age of most recent eruption

The youngest episode, including activity perhaps as recently as about 400 cal yr B.P. (A.D. 1550), indicates the possibility of eruptions during the 16th century. A report of an eruption occurring about A.D. 1550 was uncovered by the Smithsonian's Global Volcanism Program (Simkin and others, 1981) and discussed on their Web site (<http://www.volcano.si.edu/world>). The basis for this report is a notation in a compendium by Montessus de Ballore (1884, p. 18–19, entry No. 23), which describes the

“Última y formidable erupción del Chiriquí. La fecha no es exactamente fijada por Fuchs, quien pone el suceso á mediados del siglo XVI.”

(Trans: The most recent substantial eruption of [Volcán de] Chiriquí. The date is not well fixed, according to Fuchs [1880, *Volcans et tremblements de terre*], who put it in the middle of the 16th century.) [bracketed information ours]

Spanish colonization since the 16th century would have brought to the area sufficient literacy and record keeping to track subsequent eruptions, so the lack of more recently recorded eruptions presumably is a consequence of volcanic quiescence, an interpretation that agrees with our stratigraphic studies.



# Volcano Hazards Assessment

The accompanying volcano-hazard-zonation map (plate 1) shows areas that could be affected by future hazardous geologic events at or near Volcán Barú. Potentially hazardous areas around Volcán Barú include those zones related to proximal and distal lahars, pyroclastic flows, lava flows, and tephra falls. Some zones are subdivided further on the basis of their relative degree of hazard.

Hazard-zone boundaries derive from two main factors. First is the magnitude of each type of event common at the volcano, as inferred from deposits. (No historical accounts are available.) The second factor is our application of lessons learned from similar volcanic events at other volcanoes. In the case of lahars, this knowledge is quantified by an empirical model that calibrates lahar-inundation limits on the basis of

lahars of known volume that occurred elsewhere.

Individual events typically affect only part of a hazard zone. The location and size of an affected area within a hazard zone will depend on the location of the erupting vent or landslide, the volume of material involved, and the character of the eruption, especially its explosivity.

Although sharp boundaries delineate each hazard zone on the maps, the limit of the hazard does not change or end abruptly at the boundaries. Instead, the hazard decreases gradually as distance from the volcano increases. For lahars, the hazard decreases rapidly with increasing elevation above valley floors. Areas immediately beyond distal hazard zones are not free of risk, because the hazard limits can be located only approximately, especially in areas of low relief. Uncertainties about the source, size, and mobility of future eruptive phenomena preclude a precise location for the hazard zone boundaries.

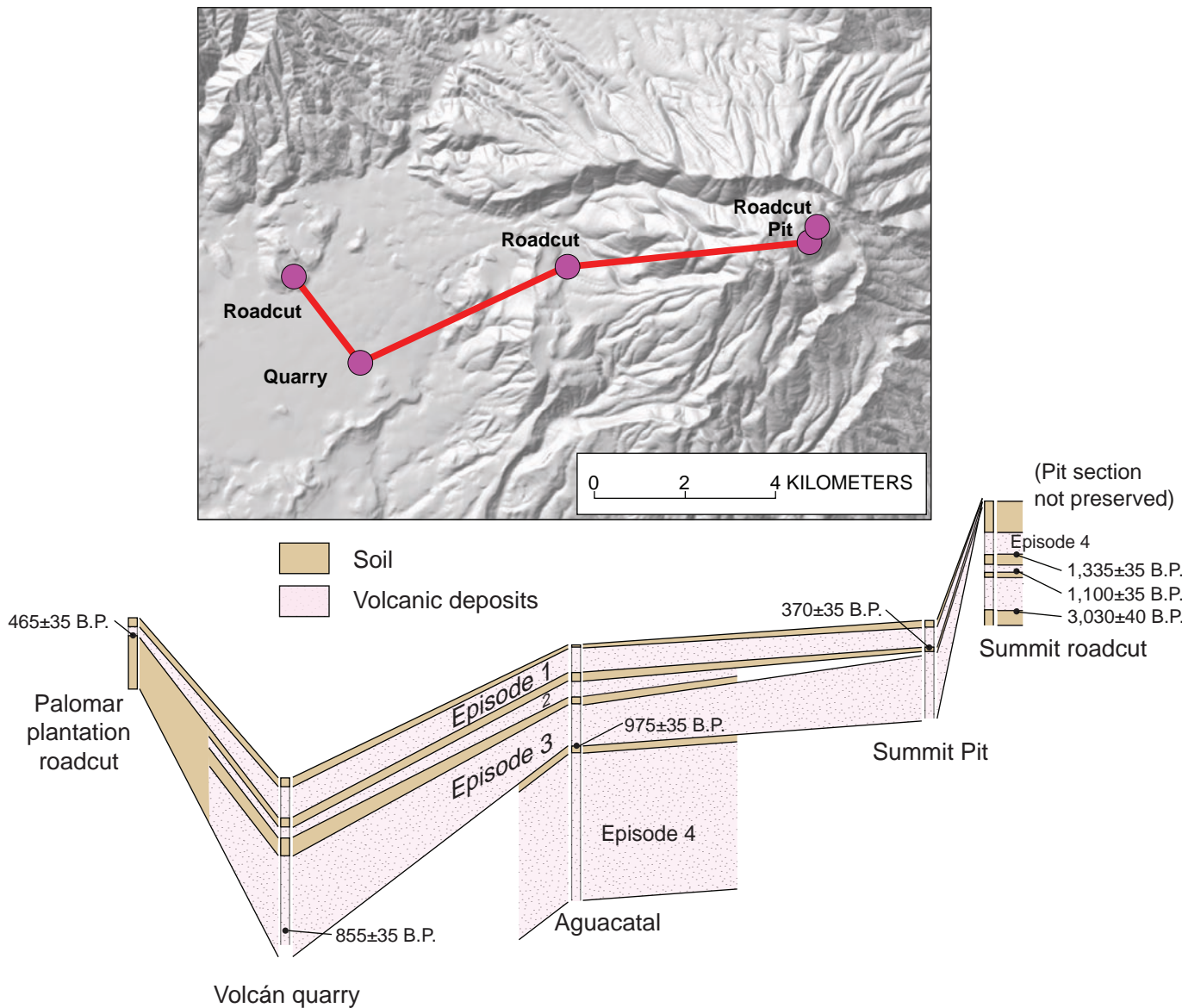


**Figure 11.** Fence diagram showing schematic distribution of paleosols and volcanic deposits for five sites at Volcán Barú. Sequence at Volcán quarry is illustrated in figure 13. Sequence at Aguacatal is detailed in table 3.

## Tephra-fall hazards

Distribution of fallout tephra from future explosive eruptions will be a consequence of the size of the eruption, altitude of the eruptive cloud, and direction of prevailing wind. Volcán Barú's eruptive activity of the past few thousand years has been that related to dome growth, and tephra clouds likely

have resulted from explosions that began or punctuated the dome-building episodes. Eruptive clouds associated with most future dome growth will ascend to about 10,000 m or less. A few of the more explosive eruptions could send tephra higher, but their probability is substantially less.

To determine prevailing wind patterns for this study, we drew upon ten years of data, from January 1997 to

**Table 3.** Interpretive stratigraphic section of Aguacatal site, 4.6 km west of Barú summit.

[Possible age spans for eruptive episodes, in calibrated years B.P., from ages compiled in figure 12 and tables 1 and 2. Dormant periods shown as duration, in years.]

Eruptive status	Age or inferred time interval	Interval thickness, in cm	Unit description	Inferred style of volcanism at site	Related <sup>14</sup> C ages
Dormant	400–500 yr	5	Soil	Quiescent interval	
Eruptive episode 1	Sometime between 420 and 540 cal yr B.P.	7	Lithic lapilli	Lithic tephra fall	370±35 at summit saddle, 420±30 at Florentina plantation, 465±35 at Palomar plantation roadcut
		12	Fine ash	Pyroclastic surge fallout	
		15	Bedded fine to very coarse ash layers	Pyroclastic surge	
		12–20	Pumice lapilli	Pumiceous tephra fall	
		3	Very fine ash	Pyroclastic surge fallout	
Dormant	<250 yr	20	Paleosol (buried soil)	Quiescent interval	
Eruptive episode 2	Undated	12	Very fine ash	Pyroclastic surge fallout	Undated
		5	Fine to medium ash	Pyroclastic surge	
		18	Very fine to fine ash	Pyroclastic surge fallout	
Dormant	<250 yr	15	Paleosol	Quiescent interval	
Eruptive episode 3	Sometime between 690 and 950 cal yr B.P.	10	Very fine to very coarse lithic ash	Pyroclastic surge	855±35 at Volcán quarry
		20	Very coarse ash and lithic lapilli	Pyroclastic surge or blast	
		2	Very fine ash	Pyroclastic surge fallout	
		15	Fine to very coarse ash and lithic lapilli	Pyroclastic surge	
		7	Very fine to fine ash	Pyroclastic surge fallout	
		36	Fine to very coarse ash and lithic lapilli	Pyroclastic surge	
		4	Very fine ash	Pyroclastic surge fallout	975±35, this unit at this site
		3–4	Pumice lapilli	Pumiceous tephra fall	
Dormant	230–620 yr	15	Paleosol	Quiescent interval	
Eruptive episode 4	Sometime between 1,180 and 1,310 cal yr B.P.	17	Fine ash	Pyroclastic surge fallout	1,100±35 or 1,345±30 at summit roadcut
		25	Medium to very coarse pumiceous and lithic ash	Pumiceous tephra fall	
		100–150	Fine to coarse ash with lithics to 20 cm and rounded pumice lapilli	Pyroclastic flow	
		40		Pyroclastic surge fallout	
		100+		Pyroclastic flow	

December 2006. The raw wind data are from the U.S. National Oceanographic and Atmospheric Administration Web site (<http://www.arl.noaa.gov/ss/transport/archives.html>). A computer program (Ewert and others, 2003) gathers data from the archives for a given latitude and longitude. The program extracts data from the three grid points nearest the point of interest and computes a distance-weighted average of the data.

The results illustrate the northeast or east orientation for prevailing winds (wind blowing from the Caribbean to the Pacific side of Panamá) (fig. 14). Shear at high altitude (above about 16,000 m) produces westerlies and easterlies in almost equal proportion. In the dry season (roughly January through April), the wind at height 9,000–14,000 m is from the south and southwest (from Pacific to Caribbean).

The zone for tephra fallout hazards is defined on the basis of the size and distribution of past fallout deposits (fig. 4) and the prevailing wind direction likely to affect future eruptions. As a guide to further delineating tephra fall hazard zones, hypothetical tephra-fallout patterns can be projected on the basis of programs derived from known tephra fallout at other volcanoes, using the characteristic prevailing wind for Volcán Barú, erupted volume, and eruptive column height. Examples

are shown for a  $5 \times 10^6 \text{ m}^3$  eruption during wet and dry seasons (fig. 15).

Substantial tephra (accumulations 10 cm to several meters thick) may fall on the summit and upper flanks, but these sites are uninhabited. Downwind sites have more infrastructure at risk. Mid-altitude winds (7.6–12.4 km) in the Volcán Barú area blow toward the west and southwest 40 percent of the time. Volcán town is the settlement most likely to be downwind during eruptions and lies within the zone for which tephra from most eruptions would likely accumulate to 5–10 cm. Similar thicknesses could fall in Cerro Punta or Boquete, but suitable wind directions occur much less frequently.

## Pyroclastic-flow hazard zones

The hazard with greatest threat to human life will be pyroclastic flows that accompany renewed dome growth during future eruptions. If eruptions are at the summit, the pyroclastic flows will move westward, owing to the configuration of the volcano's westward-opening amphitheater. Many will proceed onto the plain that underlies

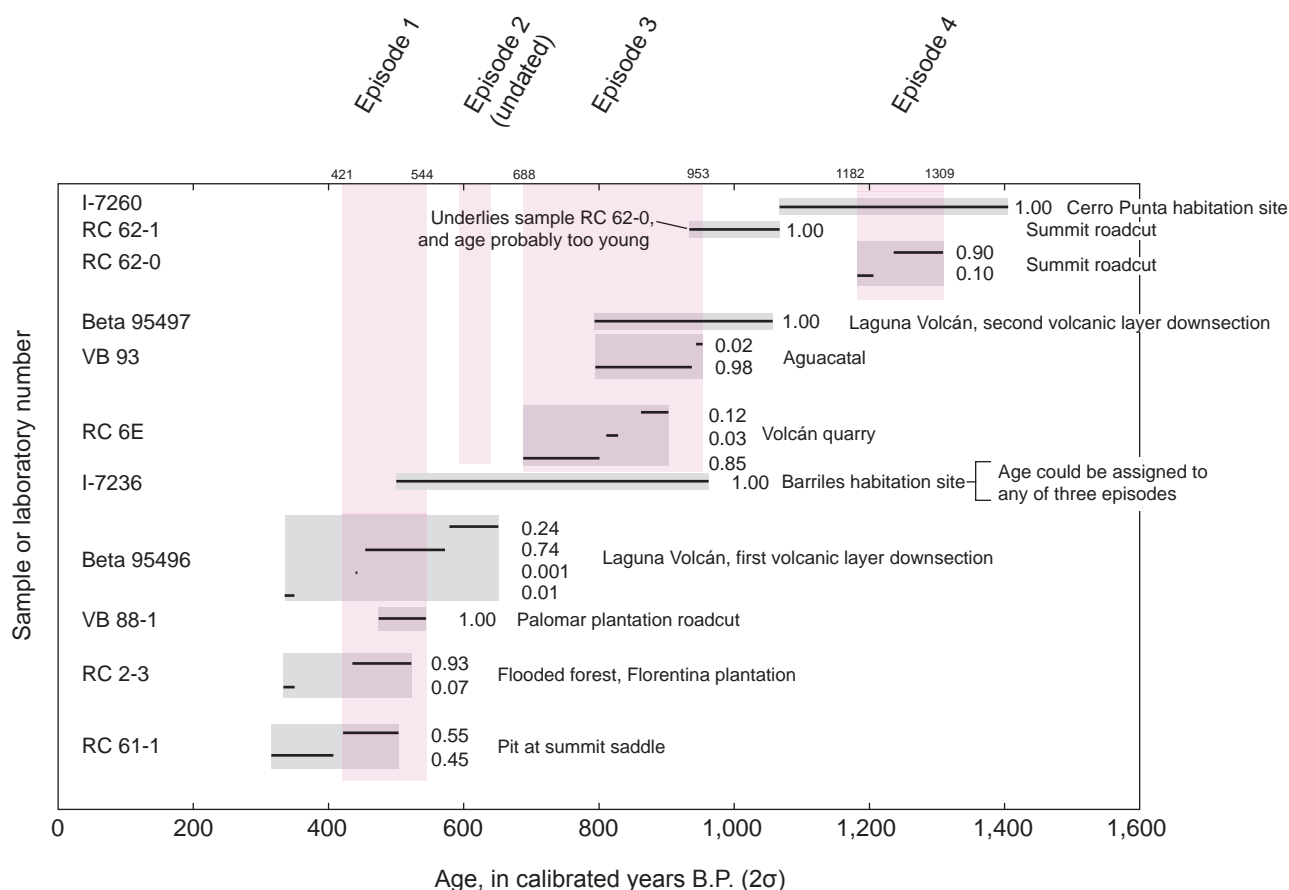


**Figure 12.** Calibrated ages of the past 1,600 years. Ages with “Beta” prefix from Behling (2000); those with “I” prefix from Linares and others (1975); all others are data newly reported here. Locations shown on figure 11. Gray box, each sample; horizontal bars, calibrated ranges; numbers on right, probability. Pink bars depict episodes as interpreted qualitatively from combination of radiocarbon ages and sequences of paleosols.



Nuevo Bambito and Volcán town. The main body of each flow will be a dense granular flow constrained by topographic barriers. Of those headed west, only the largest will enter the Río Chiriquí Viejo or Río Macho de Monte and escape beyond the area of Volcán town. A few pyroclastic flows may enter the Río Bregue and Río Chaspa, which have breached the amphitheater’s south rim.

Ash clouds will accompany many or most of the pyroclastic flows. The ash in these low-density clouds, lofted above the main body of the pyroclastic flows, will advance 1–5 km beyond those flows and be deposited in beds less than 3 cm thick.

### An eruption north or east of the volcano’s rim brings increased threat to Boquete

The summit dome need erupt only a few hundred meters east of the summit or grow only slightly until its products could overtop the east amphitheater rim. Thereafter, pyroclastic flows could descend the volcano’s east flank, conceivably reaching as far as Boquete, Alto Boquete, and the Río Caldera. Unlike the volcano’s west flank, the east flank is creased by numerous canyons that would funnel block-and-

ash flows into drainages and preserve midslope areas from inundation. The east flank is steeper, however, so dilute ash clouds that roil up there may travel farther and impact greater areas with deposits of fine ash several centimeters thick.

### Lahar hazard zones

Users of the hazard map should be aware that we have not exhaustively simulated all potentially hazardous landslide and lahar areas. The edifice of Volcán Barú is steep and incised, and its ancient edifice-collapse amphitheater will influence the amount of material available for future lahars by controlling the distribution of many volcanic deposits. For this report, we selected prominent channels directed toward populous areas in order to define the most significant paths of inundation from lahars of various volumes. Other channels, though not modeled for lahar inundation, have some lahar hazard. Landslides and lahars in them could threaten life and property.

### Proximal lahar-hazard zones

The proximal lahar-hazard zone includes areas immediately surrounding Volcán Barú and extends 2 to 6 km

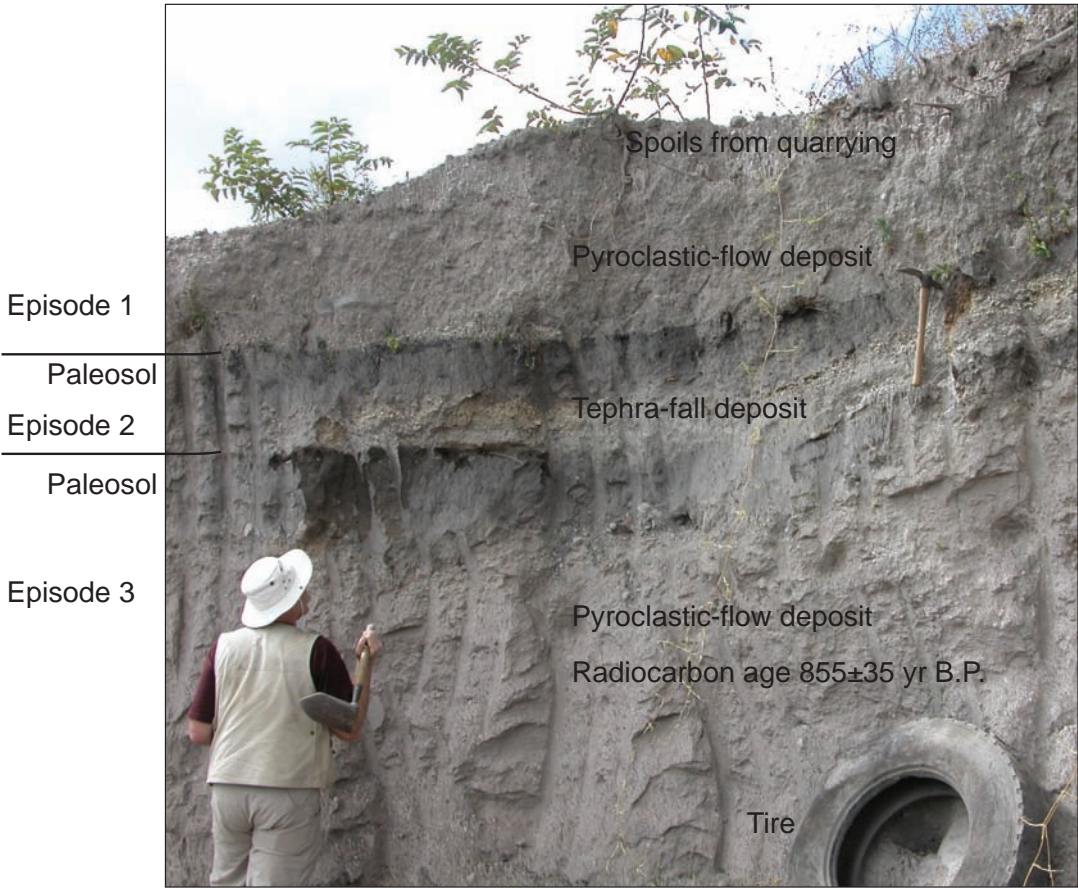


**Figure 13.** Exposure of pyroclastic-fall and -flow deposits in Volcán quarry. Dark-gray paleosols developed on tephra-fall and pyroclastic-flow deposits. Charcoal within lower deposit yielded an age of 855±35 <sup>14</sup>C yr B.P. (table 1). Thin pyroclastic-flow deposit buries upper paleosol. Uppermost layer disturbed during quarrying. Similar view elsewhere in same quarry is in figure 5B. Episode numbers correspond to those in figures 11 and 12.

outward from the summit depending upon local topography (plate 1). This zone delineates areas where lahars originate. During periods of volcanic unrest or during an eruption, this area should be evacuated because events can occur too quickly for humans to escape harm. Avalanches and lahars will originate in the proximal area, and deposits from small slides and flows may be restricted to this zone. However, large debris avalanches and lahars will travel away from the volcano and flow over broad areas. The extent of inundation from larger lahars is the basis for defining distal lahar-hazard zones.

## Distal lahar-hazard zones

An automated empirical technique, LAHARZ, calibrated with data from other volcanoes (Iverson and others, 1998; Schilling, 1998), estimates potential areas of inundation from future lahars of various volumes. For each channel analyzed, we show three to four nested hazard zones that depict anticipated inundation by hypothetical lahars of

different volumes. The largest lahar volume chosen reflects our estimate of the largest probable lahar generated on the steep slopes that head on the central vent of Volcán Barú (plate 1). The intermediate and smallest lahars are more typical and may originate anywhere on the slopes of the volcano if unusually intense rainstorms occur. Even the smallest lahars, with relatively short runout distance, can be devastating to settlements on low-lying floodplains and to bridges, pipelines, and utilities that span river valleys.

The LAHARZ program distributes a specified volume of debris along a channel beginning at a user-specified starting point. Selection of starting points varied depending on setting. An “energy cone” (Iverson and others, 1998; Schilling, 1998) was used as a boundary for selecting starting points in drainages that breach the amphitheater. These drainages would have the largest volumes of debris mobilized within them during or following future eruptions. Drainages that head on the volcano’s flanks outside the amphitheater likely will host smaller lahars, simply because the sediment supply will be less. For them, only the smaller volumes were modeled, and

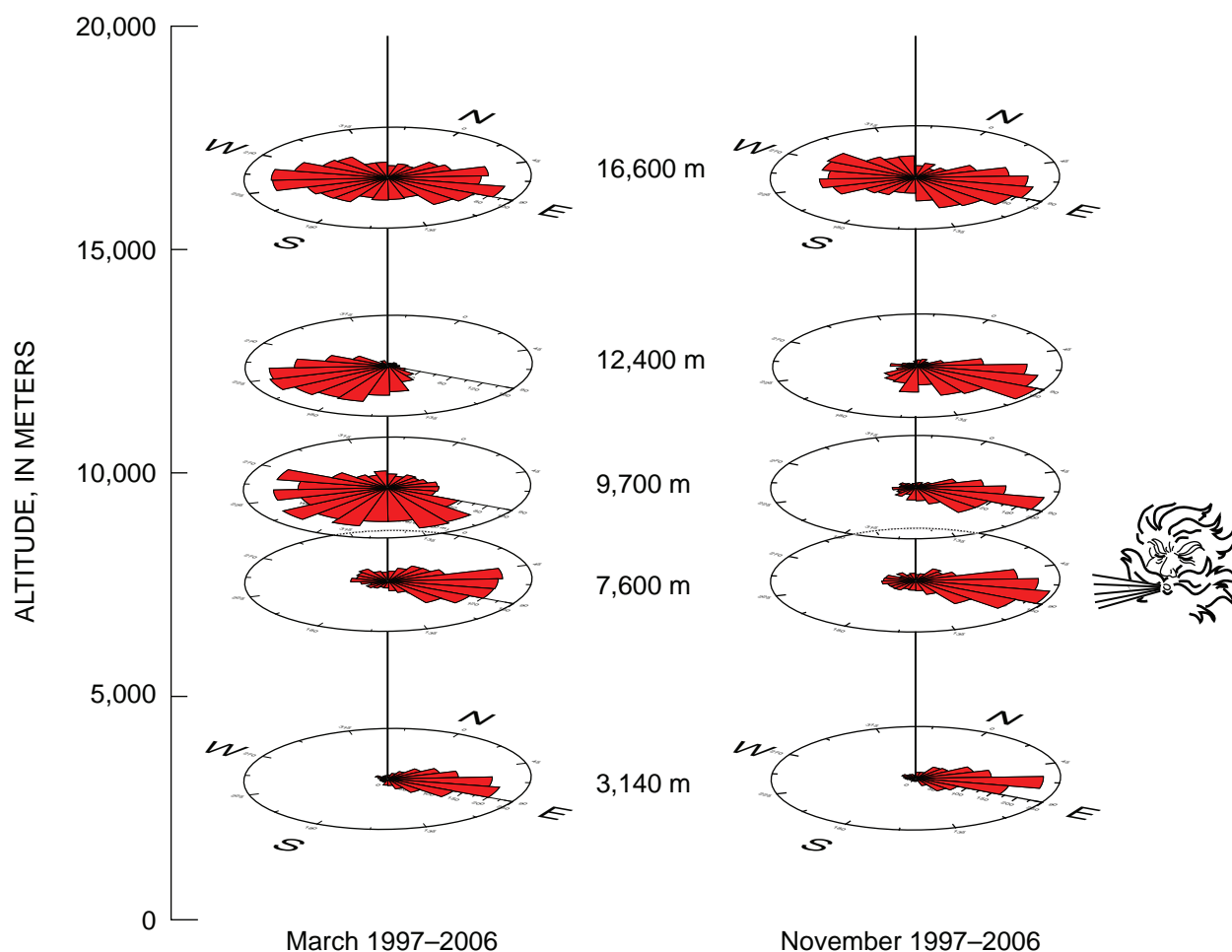


**Figure 14.** Wind rose diagrams showing direction of prevailing wind for dry (March) and wet (November) seasons, averaged from ten-year period 1997–2006. Data from National Oceanographic and Atmospheric Administration (<http://www.arl.noaa.gov/ss/transport/archives.html>). Histograms point toward the direction from which wind blows, as indicated fancifully by animated face for the November data from 7,600-m altitude.

starting points were high on the volcano's slopes. An excellent summary of the LAHARZ program as applied to other Central American volcanoes was provided by Major and others (2004, p. 96–98).

The lahar zones are worst-case scenarios for each volume chosen, because the modeled volume is emplaced instantaneously into the drainage at the specified starting point. Lahars at Volcán Barú are rainfall-induced slurries; an eruption merely provides abundant fragmental material that is gravitationally unstable and can be mobilized readily. Such lahars likely increase in volume during a storm, their runout

typically falling short of the maximum inundation that might be seen had the total volume been sudden in its onset.

In general, lahar hazard zones extend 10 to 20 km from the summit, but a few reach farther (plate 1). Topography along route plays a large role in controlling the distances that lahars travel. Although lahars originate in and flow along steeply incised drainages on the flanks of the volcano, these channels shallow and flatten out along alluvial fans west and south of the volcano. As a result, lahars spill from channels, spread, and stop. The most distant hazard zones are at the downstream reach of the most deeply incised channels, those in which lahars will remain confined for greater distances.

Drainages can become so choked with volcanoclastic sediment from lahars and pyroclastic flows that channels fill with sediment and switch course. When channels change, hazards in the new channel are greatly increased owing to the abundant unstable material that subsequently fills them.

## Lava-flow hazard zones

Lava flows from the summit area likely would remain trapped within the ancient collapse amphitheater or extend slightly beyond it on the Volcán plain. These flows would advance slowly as thick viscous masses. Greatest hazard is for collapses from their snout or flanks, which would generate small block-and-ash flows downslope. In gently sloping areas, the runout distance may be only a few tens of meters, whereas in steeper terrain the runout could traverse a kilometer or more.

The area encompassing lava-flow hazards would need to be modified if the eruption began outside of the amphitheater. In that case, areas 5–15 km downslope from the vent would lie within some redefined lava-flow hazard zone that would be drawn on the basis of the vent location. Similarly, the zone would need to be redefined if dome growth overtopped the low points on the amphitheater rim.

## A Note about Remote Sensing

One of the most powerful volcano-monitoring tools developed in the past decade has been the use of Synthetic Aperture Radar (SAR) imagery, obtained from satellites, to create interferograms showing ground deformation. At composite volcanoes, the interferograms commonly display a bullseye pattern owing to increasing amounts of deformation in the area above a magmatic conduit. Ground displacements as small as a few centimeters can be recognized by the method of differencing two images taken over a period of days, weeks, or months. However, if too much time passes in the sequence, the coherence between imagery lessens too greatly to be of value for this technique.

Coverage of Volcán Barú by the C-band (radar wavelength of 5.7 cm) ENVISAT satellite is sparse, so much so that suitable pairs of images are unavailable. Also, the dense vegetation on the north, east, and south flanks of the volcano

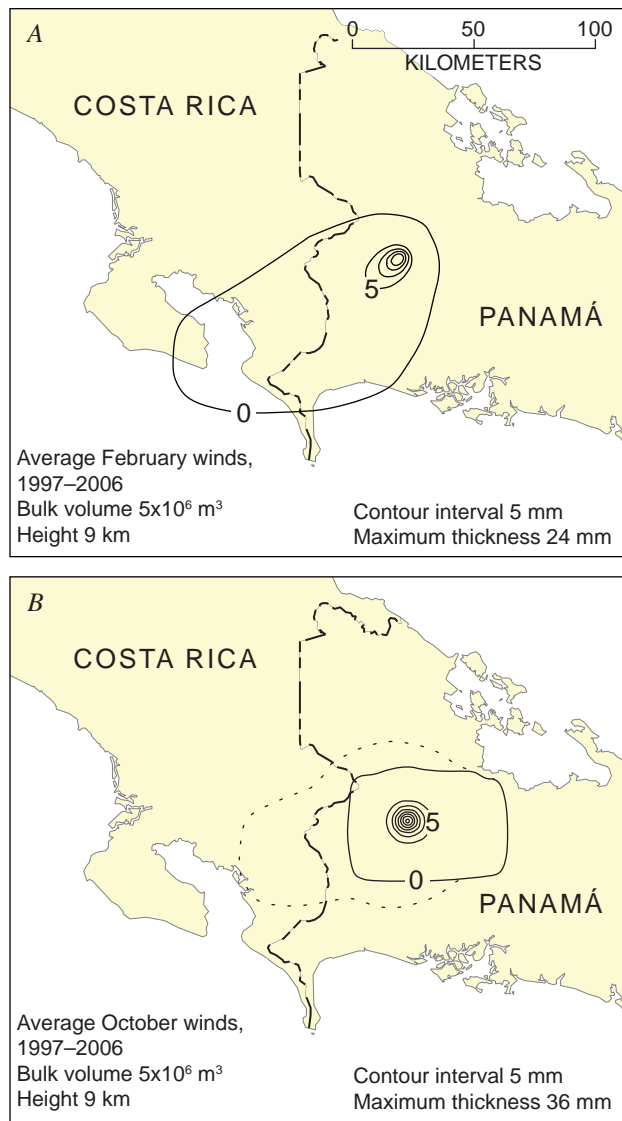


**Figure 15.** Hypothetical tephra fallout from 5-million-cubic-meter eruption at Volcán Barú. Differing distribution is consequence of changes in prevailing wind direction and strength at different altitudes. Data from U.S. National Oceanographic and Atmospheric Administration. *A*, Dry season, average February winds; *B*, Wet season, average October winds. Dotted contour (on *B*) is zero thickness line for a 25 million-cubic-meter eruption that reaches to 14 km height.



reduces the likelihood that ENVISAT imagery could produce useful interferograms. The newer ALOS satellite imagery, which uses an L-band radar for sensing (wavelength of 23.6 cm), is more promising in densely vegetated areas, but no coverage was obtained for 2006 when the recent earthquake swarm occurred. Unvegetated or sparsely vegetated areas, including the summit dome and lower west flank, may produce useful interferograms from both C-band and L-band satellite radar imagery.

The U.S. Geological Survey has acquired L-band imagery from the ALOS database for Volcán Barú and is undertaking an effort to check for coherency between successive images from August and November 2007 (Zhong Lu, oral commun., Jan. 14, 2008). These actions will aid substantially in preparing for the next magmatic and seismic activity at Volcán Barú.

## Acknowledgments

Work at Volcán Barú benefited by logistical assistance and support from Julio Escobar (National Secretariat for Science, Technology and Innovation (SENACYT) of the Republic of Panamá), Chris Cushing and Kermit Moh (U.S. Agency for International Development), and Eduardo Camacho (University of Panamá). Camacho and Randy White (USGS) provided additional information about past seismic events. We were assisted in field work by Silka Lasso (Ciudad David) and Eric Chichaco (Univ. Panamá). Félix Saldaña (local office of the National Environmental Authority) provided permission to collect samples in the Volcán Barú National Park. Our informal host proved to be Angel Rodriguez, whose collaboration allowed us to double the accomplishments of 12 field days. Tephra fallout modeling by John Ewert and LAHARZ program support and training by Steve Schilling (both USGS) were critical during the writing of this report. Lee Siebert (Smithsonian Institution, Global Volcanism Program) cheerfully made available substantial library resources. Tom Gardner (Trinity University, San Antonio, Texas), Kristen Morell and Don Fisher (Penn State University), and Hugh Cowan (New Zealand Earthquake Commission) shared freely of their unpublished radiocarbon data. The summary of remote-sensing data stemmed largely from research by Zhong Lu and Mike Poland (USGS). This report was reviewed and improved by Willie Scott, Chris Waythomas, Phil Gelman, Jenda Johnson, Camacho, and Moh. Eduardo Camacho reviewed the spanish-language translation of part 1.

## References Cited

- Behling, H., 2000, A 2860-year high-resolution pollen and charcoal record from the Cordillera de Talamanca in Panama: a history of human and volcanic forest disturbance: *The Holocene*, v. 10, no. 3, p. 387–393.
- de Boer, J.Z., Defant, M.J., Stewart, R.H., Restrepo, J.F., Clark, L.F., and Ramirez, A.H., 1988, Quaternary calc-alkaline volcanism in western Panama: regional variation and implication for the plate tectonic framework: *Journal of South American Earth Sciences*, v. 1, no. 3, p. 275–293.
- Defant, M.J., Jackson, T.E., Drummond, M.S., de Boer, J.Z., Bellon, H., Feigenson, M.D., Maury, R.C., and Stewart, R.H., 1992, The geochemistry of young volcanism throughout western Panama and southeastern Costa Rica: an overview: *Journal of the Geological Society of London*, v. 149, p. 569–579.
- Ewert, J.W., Hurst, A.W., and Denlinger, R.P., 2003, Evaluating volcanic ashfall hazards in Central America [abs.], in *Cities on Volcanoes 3*, Hilo, Hawaii, July 14–18, 2003: [Hilo, HI, International Association of Volcanology and Chemistry of the Earth's Interior (IAVCEI)], Abstract volume, p. 40.
- IRHE, 1985, Estudio de prefactibilidad avanzada del complejo Barú–Colorado, informe geovulcanológico [unpub. report]: Instituto de Recursos Hidráulicos y Electrificación, Informe del Convenio IRHE-BID-OLADE, 74 p. [Smithsonian Institution, Global Volcanism Program library collection.]
- Iverson, R.M., Schilling, S.P., and Vallance, J.W., 1998, Objective delineation of lahar-hazard zones downstream from volcanoes: *Geological Society of America Bulletin*, v. 110, p. 972–984.
- Jackson, T.E., 1991, Neogene geochemistry of the Central American arc, western Panama and southeastern Costa Rica: Tampa, University of South Florida, master's thesis, 109 p.
- Le Bas, M.J., and Streckeisen, A.L., 1991, The IUGS systematics of igneous rocks: *Journal of the Geological Society of London*: v. 148, p. 825–833.
- Linares, O.F., Sheets, P.D., and Rosenthal, E.J., 1975, Prehistoric agriculture in tropical highlands: *Science*, v. 187, p. 137–145.
- Major, J.J., Schilling, S.P., Pullinger, C.R., and Escobar, C.D., 2004, Debris-flow hazards at San Salvador, San Vicente, and San Miguel volcanoes, El Salvador, chap. 7 of *Rose, W.I., Bommer, J.J., López, D.L., Carr, M.J., and Major, J.J., eds., Natural hazards in El Salvador: Geological Society of America Special Paper 375*, p. 89–108.
- Montessus de Ballore, F., comte de, 1884, Temblores y erupciones volcánicas in Centro-América, con un apéndice meteorológico: San Salvador, F. Sagrini, 246 p.
- Myers, B., Brantley, S.R., Stauffer, P., and Hendley, J.W., III, 2002, What are volcano hazards?: U.S. Geological Survey Fact Sheet 002-97, revised 2004, 2 p.
- Rausch, S., 2007, Geochemical signatures in subduction zone magmatism at Volcan Barú, Panama: Göttingen, Germany, Georg-August-Universität Göttingen, master's thesis, 110 p.
- Reimer, P.J., Baillie, M.G.L., Bard, E., Bayliss, A., Beck, J.W., Bertrand, C.J.H., Blackwell, P.G., Buck, C.E., Burr, G.S., Cutler, K.B., Damon, P.E., Edwards, R.L., Fairbanks, R.G., Friedrich, M., Guilderson, T.P., Hogg, A.G., Hughen, K.A., Kromer, B., McCormac, F.G., Manning, S.W., Ramsey, C.B., Reimer, R.W., Remmele, S., Southon, J.R., Stuiver, M., Talamo, S., Taylor, F.W., van der Plicht, J., and Weyhenmeyer, C.E., 2004, IntCal04 terrestrial radiocarbon age calibration, 26 – 0 ka BP: *Radiocarbon*, v. 46, p. 1029–1058.
- Restrepo, J.F., 1987, A geochemical investigation of Pleistocene to recent calc-alkaline volcanism in western Panama: Tampa, University of South Florida, master's thesis, 103 p.
- Schilling, S.P., 1998, LAHARZ: GIS programs for automated mapping of lahar-inundation hazard zones: U.S. Geological Survey Open-File Report 98–638, 84 p.
- Simkin, T., Siebert, L., McClelland, L., Bridge, D., Newhall, C., and Latter, J.H., 1981, *Volcanoes of the world*: Stroudsburg, Penn., Hutchinson Ross Co., 232 p. [After two printed editions, 1981

- and 1994, this resource has become the online, frequently updated publication “Volcanoes of the world,” accessible at <http://www.volcano.si.edu/world>. Last accessed November 2007].
- Siebert, L., Alvarado, G.E., Vallance, J.W., and van Wyk de Vries, B., 2006, Large-volume volcanic edifice failures in Central America and associated hazards, chap. 1 of Rose, W.I., Bluth, G.J.S., Carr, M.J., Ewert, J.W., Patino, L.C., and Vallance, J.W., eds., *Volcanic hazards in Central America: Geological Society of America Special Paper 412*, p. 1–26.
- Siebert, L., Kimberly, P., and Pullinger, C.R., 2004, The voluminous Acajutla debris avalanche from Santa Ana volcano, western El Salvador, and comparison with other Central American edifice-failure events, chap. 2 of Rose, W.I., Bommer, J.J., López, D.L., Carr, M.J., and Major, J.J., eds., *Natural hazards in El Salvador: Geological Society of America Special Paper 375*, p. 5–23.
- Stewart, R.H., 1978, Preliminary geology, El Volcan region, Province of Chiriquí, R[epublic] of P[anama] [unpub. report]: Washington, D.C., Smithsonian Institution Libraries, item No. (bar code) 39088007923337, Library of Congress Classification GB/1199.8/. P2 S85/1978, Smithsonian Tropical Research Institute, 27 p. plus 8 figures, 27 photos, and 2 appendices, variously paginated.
- Stuiver, M., and Reimer, P.J., 1993, Extended  $^{14}\text{C}$  database and revised CALIB radiocarbon calibration program: *Radiocarbon*, v. 35, p. 215–230.
- Terry, R.A., 1956, Geological reconnaissance of Panama: San Francisco, California Academy of Sciences Occasional Paper 23, 91 p.
- Universidad Tecnológica de Panamá, 1992, Evaluación de la amenaza, estimación de la vulnerabilidad y del factor costo del riesgo del Volcán Barú, Republica de Panamá: Departamento de Geotécnica Facultad de Ingeniería Civil, Universidad Tecnológica de Panamá, con apoyo del Centro para la Prevención de Desastres Naturales en América Central (CEPREDENAC), 129 p., 2 pls., escala 1:100,000.

## Appendix 1. Chemical analyses

Whole-rock samples were collected from lava flows, including the summit dome, and as pumice lumps from tephra-fall deposits. Major and trace element analyses (table 4) were determined by X-ray fluorescence spectroscopy using an automated ThermoARL model Advant'XP Plus spectrometer at Washington State University Geoanalytical Laboratories. Accuracy and precision are discussed fully on their Web site, <http://www.wsu.edu/~geolab/note/xrfprecision.html>. Analytical precision for major elements is generally better than 1 percent of the oxide value reported here. For the trace elements, precision is better than 10 percent and commonly in the range 3–5 percent of the reported value. The following elements have precision of about 25 percent: La, Nb, Pb, Ce, and Nd. Thorium, present in very low amounts, has precision of about 50 percent.

We also compiled analyses from the published and unpublished literature (table 5). The two largest collections were in master's theses (Restrepo, 1987; Rausch, 2007). Added to the Restrepo samples are additional trace-element analyses (Jackson, 1991) and a few Sr and Nd isotopic ratios (Jackson, 1991; Defant and others, 1992).

Location data in table 5 vary greatly in quality. We used a handheld GPS receiver or, in rare cases, determined our sample locations by inspection using topographic maps where the latter method produced better accuracy. Precision shown by the GPS receiver was generally 5–15 m, which corresponds roughly to accuracy of 15–50 m as estimated by repeated survey of known points on successive days. Locations for the analyses from past reports were digitized using sample location maps. These maps were at small scale; consequently the accuracy varies greatly and may exceed 100 m. One of the reports had maps at two scales, and locations differed by as much as 1.1 km between them, far outside the 100-m shift that might arise from projecting maps in the two common datums WGS84 and NAD27 Canal Zone. None of the reports

had sample-description pages that allowed us to determine the geologic unit sampled, so we relied on locations alone for stratigraphic assignments shown in table 5.

## Appendix 2. Reconstruction of the precollapse cone and volume of debris avalanche

We estimate the volume of the debris avalanche by two different approaches. The first is to estimate the surface configuration of the precollapse volcano, calculate the volume contained by that volcanic edifice, and then subtract from it the modern edifice. Using GIS, this source-area volume can be calculated by contouring and gridding the estimated precollapse and modern surfaces to determine the volume bounded by them. The other approach is to estimate the area and thickness covered by the debris-avalanche deposits.

The precollapse edifice is reconstructed by projecting the existing topographic contours across the area now occupied by the amphitheater. The precollapse volcano is symmetrical across its east, south, and southwest parts, as can be shown by superimposing circles whose diameters approximate the trace of specific contour lines (fig. 16A). The circles have centers that lie within 700 m of each other, all centered close to the modern summit. These circles provide the guidelines for resurrecting the surface of the precollapse volcano (fig. 16B). This reconstruction treats the ancestral summit as a dome complex, much like the modern summit; highest altitude is 3,800–3,900 m in this reconstruction. The circular nature of the contours belies the visual illusion that the ancestral volcano was elongate east-west, an illusion created by the amphitheater's configuration. Some reports describe east-west-trending structures in the cone (for example, Restrepo, 1987); but we found neither dikes nor topographic lineaments along

**Table 4.** Analyses showing new major- and trace-element concentrations in Quaternary volcanic rocks from Volcán Barú, Republic of Panamá.

[Arranged in order of roughly decreasing age, to match table 5. See table 5 for geographic, stratigraphic, and lithologic information. Analyses by X-ray fluorescence at Geoanalytical Labs, Washington State University, Pullman, Wash. Also shown are normalized SiO<sub>2</sub> values, all iron as Fe<sup>2+</sup>.]

Sample No.	S07-VB07	S07-VB46B	S07-VB47	S07-VB52	S07-VB55	S07-VB58	S07-VB81B	S07-VB101	S07-VB01	S07-VB103	S07-VB104
<b>Major-element analyses (weight percent)</b>											
SiO <sub>2</sub>	60.24	63.02	57.53	58.75	58.16	58.52	54.82	55.62	55.61	58.05	57.75
TiO <sub>2</sub>	0.601	0.405	0.711	0.631	0.640	0.600	1.040	0.763	0.749	0.661	0.652
Al <sub>2</sub> O <sub>3</sub>	17.16	17.47	16.85	17.39	17.47	17.45	17.79	16.55	18.09	17.60	17.47
FeO	4.95	3.31	5.88	5.41	5.23	5.70	6.88	6.55	6.58	6.48	6.35
MnO	0.092	0.065	0.104	0.101	0.092	0.107	0.128	0.122	0.120	0.123	0.126
MgO	3.19	2.23	3.39	3.01	3.97	3.33	4.16	5.30	3.38	3.62	3.59
CaO	6.41	5.05	7.54	6.95	6.92	7.23	7.56	8.23	8.47	7.23	7.33
Na <sub>2</sub> O	4.01	4.59	3.00	3.76	4.07	3.28	3.86	3.25	3.06	3.17	3.18
K <sub>2</sub> O	1.84	1.61	2.40	1.91	1.40	1.96	1.57	1.87	1.88	1.93	1.92
P <sub>2</sub> O <sub>5</sub>	0.207	0.151	0.241	0.204	0.230	0.187	0.420	0.257	0.257	0.172	0.175
Total	98.19	98.94	97.43	98.69	97.91	97.65	98.12	98.17	98.19	99.04	98.54
SiO <sub>2</sub> , normalized to 100%, water- free	61.04	64.37	58.92	59.88	59.25	59.49	55.81	56.46	56.64	58.61	58.61
<b>Trace-element analyses (parts per million)</b>											
Sc	13	8	17	12	14	14	16	21	15	17	18
V	147	90	190	170	160	170	196	206	210	203	195
Cr	59	53	34	30	100	20	88	150	22	25	23
Ni	39	26	24	22	61	27	45	47	17	24	23
Cu	143	45	126	128	105	135	85	86	150	240	149
Zn	68	57	66	68	69	65	86	72	82	68	71
Ga	19	19	21	21	20	20	20	19	20	19	19
Rb	36	37	40	32	24	32	26	44	29	37	36
Sr	1133	1328	1477	1444	1160	1395	1093	1387	1810	1064	1098
Zr	111	91	125	104	105	95	150	142	102	98	97
Nb	6.1	5.5	4.8	4.5	7.3	3.7	11.5	6.1	4.3	3.3	3.8
Ba	1021	1385	1056	1017	888	846	830	1221	1124	907	923
Pb	6	8	7	4	5	8	5	6	7	6	7
Y	8	6	11	9	9	10	16	11	9	12	12
La	25	18	22	21	23	16	35	33	28	13	13
Ce	41	28	53	42	41	25	70	63	46	26	28
Th	3	1	4	3	2	2	4	5	4	2	1
Nd	17	11	22	19	18	13	30	26	21	13	14



**Table 4.** Analyses showing new major- and trace-element concentrations in Quaternary volcanic rocks from Volcán Barú, Republic of Panamá—Continued.

Sample No.	S07-VB108	S07-VB59	S07-VB105	S07-VB107	S07-VB04G	S07-VB06F	S07-VB601p	S07-VB602p	S07-VB603p	S07-VB88-2	S07-VB93-1p
<b>Major-element analyses (weight percent)</b>											
SiO <sub>2</sub>	58.50	61.67	63.25	59.75	61.24	59.27	59.26	58.90	60.16	59.67	58.03
TiO <sub>2</sub>	0.647	0.577	0.480	0.618	0.589	0.621	0.608	0.650	0.557	0.555	0.612
Al <sub>2</sub> O <sub>3</sub>	17.52	17.05	16.78	17.21	17.17	17.08	17.03	16.88	17.00	16.87	16.77
FeO	6.33	4.43	3.66	5.10	4.55	5.00	5.00	5.36	4.54	4.57	5.18
MnO	0.121	0.086	0.067	0.096	0.086	0.095	0.091	0.098	0.087	0.089	0.098
MgO	3.50	2.53	2.26	3.26	2.81	3.08	3.27	4.04	2.91	2.74	4.12
CaO	7.18	5.97	5.23	6.66	6.10	6.37	6.39	6.84	6.10	6.02	6.77
Na <sub>2</sub> O	3.19	4.12	4.72	3.93	4.20	3.83	3.90	3.80	3.97	3.89	3.72
K <sub>2</sub> O	1.95	2.22	1.45	1.80	1.97	1.86	1.82	1.75	1.88	2.03	1.70
P <sub>2</sub> O <sub>5</sub>	0.181	0.233	0.165	0.216	0.232	0.228	0.214	0.223	0.204	0.207	0.202
Total	99.12	98.90	98.06	98.65	98.94	97.43	97.58	98.53	97.40	96.62	97.19
SiO <sub>2</sub> , normalized to 100%, water- free	59.02	62.36	64.50	60.57	61.89	60.83	60.72	59.78	61.76	61.75	59.70
<b>Trace-element analyses (parts per million)</b>											
Sc	17	9	9	13	10	12	12	14	11	12	14
V	190	123	103	149	126	148	150	160	129	133	155
Cr	23	40	47	69	58	55	64	111	63	41	135
Ni	24	28	22	32	34	32	41	57	32	28	60
Cu	109	125	64	116	57	97	89	101	45	95	56
Zn	63	68	60	69	64	72	69	69	68	65	67
Ga	19	19	19	19	19	20	20	20	19	20	19
Rb	36	48	25	37	43	39	36	35	39	42	35
Sr	1092	1318	981	1111	1225	1160	1133	1080	1123	1170	1043
Zr	97	143	98	114	131	120	113	112	117	123	107
Nb	3.2	7.9	5.3	6.5	7.9	6.4	5.4	6.1	6.3	6.7	5.3
Ba	930	1175	791	979	1111	1028	1012	953	1036	1068	914
Pb	6	7	5	5	6	5	6	5	7	6	6
Y	12	8	6	8	8	9	8	9	8	9	9
La	17	31	12	23	25	26	23	24	21	24	19
Ce	26	56	28	43	53	48	41	43	39	42	41
Th	2	5	2	4	5	4	4	2	4	4	3
Nd	12	21	13	18	22	21	16	19	17	17	18

**Table 5.** Spreadsheet compilation of new and previously published analyses from Quaternary volcanic rocks at Volcán Barú. (Table 5 is a separate electronic spreadsheet, Barú\_chem\_all, and only representative introductory data columns shown here.)

[Column labeled “References” is keyed to References Cited in body of report. Column labeled “Volcano” shows assignment to respective volcanic edifices of Volcán Barú, Volcán Tisingal, or a sample of uncertain assignment, labeled “Regional.” Column for volcanic stage aids when sorting data stratigraphically for comparisons and temporal trends, but note that stage 2 comprises avalanche-debris material derived from stage 1 strata: 1, pre-collapse volcanic edifice; 2, block from debris avalanche deposits; 3, older pyroxene andesite that underlies summit dome; 4, summit dome; 5, pumice from deposits of past 1,600 years. Locations in decimal degrees latitude and longitude (datum WGS84). Altitude is orthometric altitude, read from map sheet after plotting location and interpolated to nearest 10 m. Location quality is ranked 1 if generally better than ±30 m; quality rank 3 for locations taken from small-scale maps and possibly in error by as much as 1 km.]

Sample Number	References	Volcano	Volc. stage	Longitude WGS84	Latitude WGS84	Altitude meters	Location quality
PAN-06-141	Rausch 2007	Baru	1	-82.565036	8.834213		3
8-1	Restrepo 1987	Tisingal	0	-82.682988	8.824284		3
9-2b	Restrepo 1987; Jackson 1991	Regional		-82.545498	8.858851		3
S07-VB103	Sherrod and others (this report)	Baru	3	-82.567346	8.812801	2250	1

such a trend. Modern and precollapse surfaces are displayed as hillshade relief models (fig. 17).

Siebert and others (2004, 2006) estimated a volume of 25–30 km<sup>3</sup> for the debris avalanche using a source-area approach. We concur. Subtracting our two surfaces yields about 15 km<sup>3</sup>. To that is added the volumes of features that have been emplaced in the amphitheater after it formed: about 4 km<sup>3</sup> for the lava flows and summit dome and 6 km<sup>3</sup> for the pyroclastic fans and talus that drape the south and southwest flanks of the recent dome. The resulting volume, about 25 km<sup>3</sup>—or 20–30 km<sup>3</sup> if expressed as one significant figure—is

the in-place volume of the volcano that was excavated by the debris avalanche.

Another common method of calculating volume is by measuring the extent of the debris-avalanche deposits and estimating their thickness. The area we map as debris-avalanche deposits from Volcan Baru covers roughly 700 km<sup>2</sup> north of latitude 8°30', or roughly the latitude of the Pan-American Highway (fig. 1); it covers some unknown area farther south on the coastal plain. The deposit thickness exceeds 50 m near the source and is more than 20 m thick in the few areas where we have seen the lower contact. The

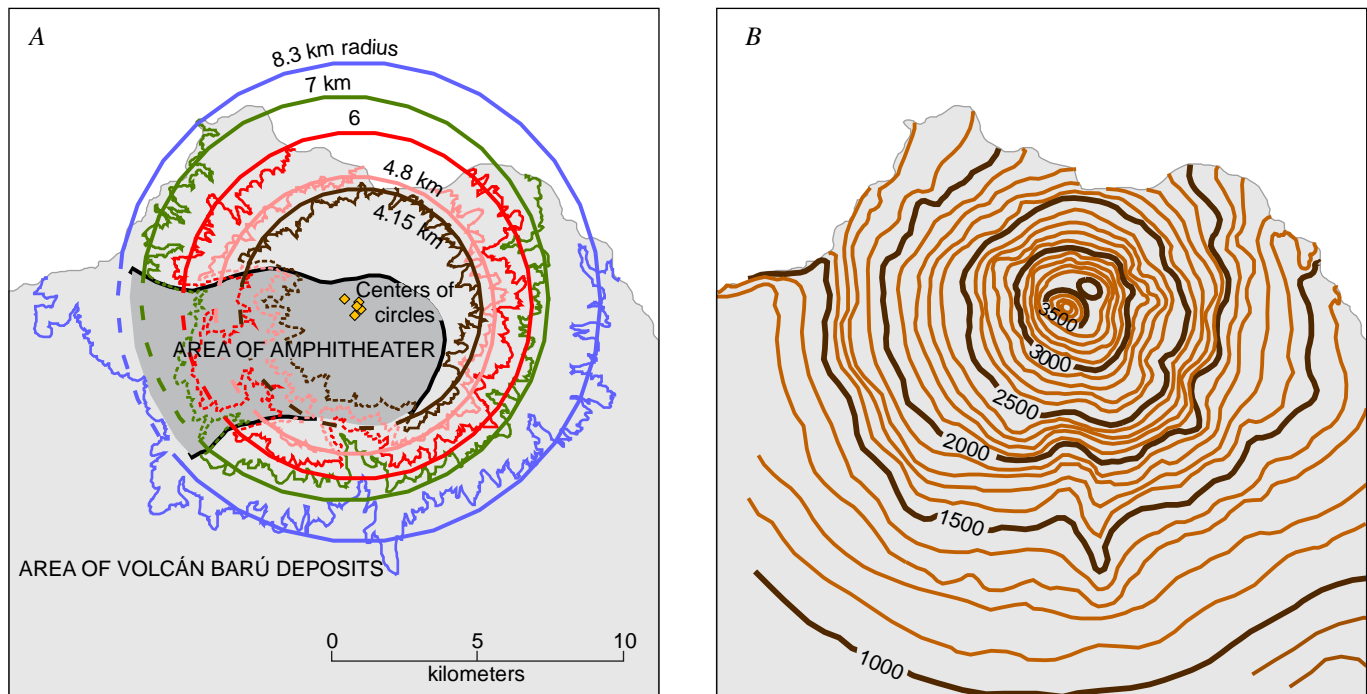


**Figure 16.** Method for determining precollapse shape of Volcán Barú. *A*, Circles as good approximations for topographic contours. *B*, Precollapse contours, showing altitude in meters.

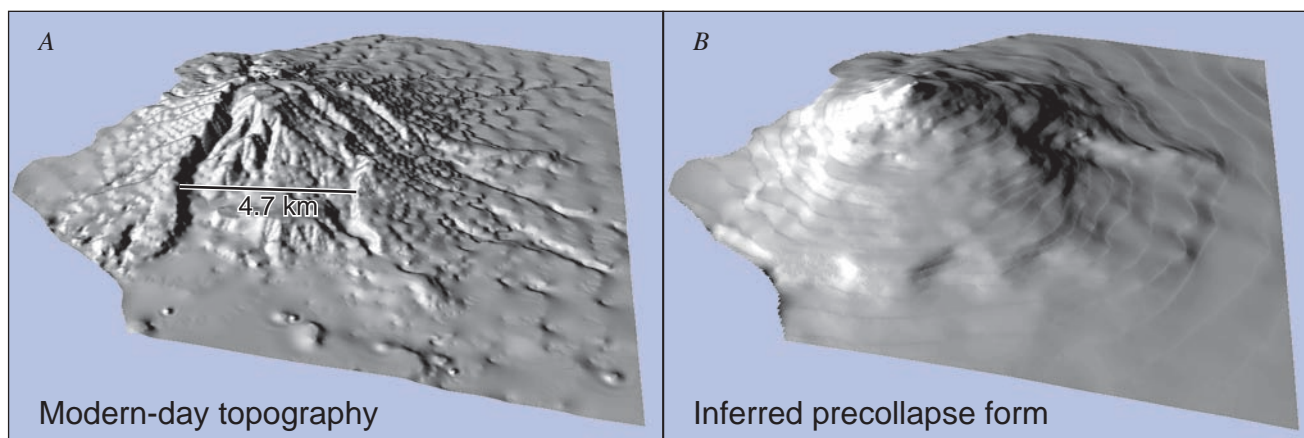


**Figure 17.** Hillslope shaded-relief images for Volcán Barú, from digital elevation models. View broadly east; north to left. *A*, modern volcano, using existing topographic contours. *B*, Prior to gutting by debris-avalanche, from contours in figure 16*B*.

reconnaissance nature of our preliminary investigation carries large uncertainties for areal extent and average thickness. A deposit volume of 25–35 km<sup>3</sup> is estimated, but the analytical error may exceed 30 percent.

### Appendix 3. Linares radiocarbon ages

Fifteen radiocarbon ages, referred to herein as the Linares ages, were published in conjunction with archaeological investigations in the area southwest and northwest of Volcán Barú (Linares and others, 1975). Dating was conducted at the Teledyne Isotopes laboratory (sample prefix I) and the Smithsonian Institution Radiation Biology laboratory (prefix SI). The stratigraphic setting of the samples appeared in an unpublished geologic report (Stewart, 1978), sketches of which were later included in an assessment of the geologic hazards of the Volcán Barú area (figs. 10A–D in Universidad Tecnológica de Panamá, 1992, p. 43–44). Of these ages, only the youngest (740±150 <sup>14</sup>C yr B.P.) has a convincing relation to primary volcanic deposits.

As best we can tell, the Linares samples were bulk soil samples collected across 10- or 20-cm depth intervals. Samples were collected from two cuts in the Barriles area. The youngest age was from sample I-7263 at 10–20 cm depth, corresponding to a stratigraphic layer described as “part pumice, part soil; medium yellow pumice.” We interpret the description thus: slightly weathered pumice lapilli admixed with soil in a zone ≤10 cm thick. The deposit is probably the youngest tephra fall preserved at that site. Whether it records the youngest volcanic event at Volcán Barú depends on the vagaries of wind at the time of a given eruption or the possibility that younger deposits have been removed or so greatly disrupted that they have gone unrecognized. The radiometric age, 740±150 <sup>14</sup>C yr B.P., has such large error that the deposit may belong to any of several volcanic events of the past 1,000 years.

The Cerro Punta site also had samples taken from two cuts. A layer of white pumice and admixed soil forms a layer at 15–30 cm depth in one cut; whereas at the other cut, nearly soil-free pumice forms a layer at 20–25 cm depth. Presumably the two pumice zones are correlative. The samples actually dated are from depths 40–50 cm and 50–60 cm, respectively, or 10–15 cm deeper than the tephra fallout zones in the two cuts. The ages are 1,635±90 and 1,350±85 <sup>14</sup>C yr B.P., from samples I-6523 and I-7260, respectively. They provide maximum ages for the overlying tephra bed, which must be younger. During our field work we recognized four major volcanic episodes occurring after the development of paleosols of 1,350 <sup>14</sup>C yr or younger by combining our knowledge of deposits, paleosols, and radiocarbon ages. The Cerro Punta young tephra-fall deposit probably correlates with the younger two or three episodes (not the oldest), in order for sufficient time to create a paleosol 10–15 cm thick above the soil sample dated from the Cerro Punta site.

The 1,350 <sup>14</sup>C-yr B.P. age (A.D. 600 if left uncalibrated) from the Cerro Punta archaeological site was interpreted by Linares and her colleagues as if it corresponded to a volcanic-event date. They concluded that “a massive eruption of Volcán Barú unquestionably terminated all human activities at Cerro Punta, around A.D. 600” (Linares and others, 1975, p. 144). We cannot judge the exodus, but if it occurred in response to the tephra bed that lies stratigraphically above the dated sample, its timing would have been sometime after and perhaps much later than A.D. 600.

### Appendix 4. New radiocarbon ages unrelated to volcanic events

To avoid confusion, the two new radiocarbon ages from samples thought unrelated to volcanic activity are listed separately (table 6) and shown parenthetically on the sample



location map (fig. 10). The younger sample is from partly charred wood in a lahar exposed in a quarry near Nuevo Bambito. The lahar is not a primary volcanic deposit. It likely resulted from weather-related events that mobilized material from block-and-ash deposits emplaced onto the Volcán fan since 1,000 years ago. These postvolcanic lahar deposits are mapped as lahars of Nuevo Bambito on the reconnaissance geologic map (fig. 8). The age is  $285 \pm 35$   $^{14}\text{C}$  yr B.P., and the calibration indicates an age most likely in the range 285–460 cal yr B.P. (table 2). Thus, the age is a limiting or minimum age for volcanic deposits in the area of Nuevo Bambito. (That is, all volcanic events in that area must be older than the age of the charred wood.)

The other age considered too young to mark a volcanologic event is from wood (not charcoal) in a roadcut west of Volcán town. We debated, during sample collection, whether the wood was a downed tree that had toppled and been buried beneath 95 cm of successive soils and tephra falls, a history that would make its age useful for volcanologic interpretation. Its radiocarbon age is  $245 \pm 35$   $^{14}\text{C}$  yr B.P., much too young for an ancient log buried that deeply; thus it appears to have been a thick subhorizontal root that had tapped down to that depth from a much younger tree. (A soil thickness less than 20–30 cm would be characteristic soil development in that geographic area during that period of time, judging from the other ages and stratigraphic depths.)

**NEXT PAGE: Table 6.** Radiocarbon and calibrated ages for samples unrelated to volcanic events, Volcán Barú, Republic of Panamá.

## Appendix 5. Location and stratigraphic setting of radiocarbon samples.

Location data for radiocarbon samples are listed in table 7, in order of increasing age. See figure 10 for location map. Subsequent illustrations (figs. 18A–H) show stratigraphic setting of the samples sites, as found in roadcuts, riverbanks, and quarries across the volcano.

**Table 7.** Locations for radiocarbon samples collected January–February 2007, Volcán Barú, Republic of Panamá.

[First two samples not related to volcanic episodes. Locations accurate to about 30 m (two to three times the stated precision of handheld GPS device). Altitude is orthometric altitude, read from map sheet after plotting location and interpolated to nearest 10 m.]

Lab No.	Sample No.	Longitude, WGS84	Latitude, WGS84	Altitude, meters	Material dated	$^{14}\text{C}$ age, yr B.P.	$\pm (1\sigma)$
WW6188	S07-VB83B	-82.6746	8.7873	1370	wood	245	35
WW6190	RC-86-1	-82.6324	8.7993	1460	charred wood	285	35
WW6166	RC-61-1	-82.5352	8.8073	3280	charcoal	370	35
WW6189	RC-2-3	-82.6313	8.8157	1530	wood	420	30
WW6162	S07-VB88-1	-82.6383	8.7996	1490	charcoal	465	35
WW6165	RC-6E	-82.6251	8.7828	1450	charcoal	855	35
WW6171	S07-VB93	-82.5843	8.8020	1990	charcoal	975	35
WW6168	RC-62-0	-82.5337	8.8103	3230	charcoal	1,345	30
WW6169	RC-62-1	-82.5337	8.8103	3230	charcoal	1,100	35
WW6167	RC-62-2	-82.5337	8.8103	3230	charcoal	3,030	40
WW6161	S07-VB56A	-82.5014	8.7965	2220	charcoal	8,340	30
WW6164	S07-VB98-2	-82.5330	8.8449	2460	charcoal	9,825	30
WW6163	S07-VB98-1	-82.5330	8.8449	2460	charcoal	13,315	40

**Table 6.** Radiocarbon and calibrated ages for samples unrelated to volcanic events, Volcán Barú, Republic of Panamá.  
[Ages calibrated to calendar years using Calib 5.0.1 software. Probabilities rounded to nearest 1 percent. Calendar ages (A.D.) unless stated otherwise.]

Lab No.	Sample No.	Material dated	$\delta^{13}\text{C}$ , per mil	$^{14}\text{C}$ age, yr B.P.	$\pm (1\sigma)$	Calibrated age B.P.			Calendar age	
						Young	Old	Probability	Young	Old
WW6188 <sup>1</sup>	S07-VB 83B	wood <sup>2</sup>	-25	245	35	-1	14	0.06	A.D. 1951	A.D. 1936
						146	189	0.26	1804	1761
						192	213	0.03	1758	1737
						268	327	0.50	1682	1623
						360	368	0.01	1590	1582
						375	429	0.14	1575	1521
						155	165	0.02	A.D. 1795	A.D. 1785
WW6190	RC-86-1	charred wood <sup>3</sup>	-25	285	35	285	338	0.35	1665	1612
						348	460	0.63	1602	1490
I-7260 <sup>4</sup>	BU-17	bulk soil organics		1,350	85	1,067	1,405	1.00	A.D. 833	A.D. 545
Beta 95499 <sup>5</sup>	126 cm depth	organic		2,860	50	2,854	3,084	0.91	905 B.C.	1135 B.C.
						3,088	3,157	0.09	1139 B.C.	1208 B.C.

<sup>1</sup> Samples with Lab prefix WW prepared at U.S. Geological Survey Radiocarbon Lab, Reston, Va., as part of this report. Ages determined on July 2, 2007, by mass spectrometric methods at the Center for Accelerator Mass Spectrometry, Lawrence Livermore National Laboratory, Livermore, Calif. Presumed value for  $\delta^{13}\text{C}$  is -25 per mil.

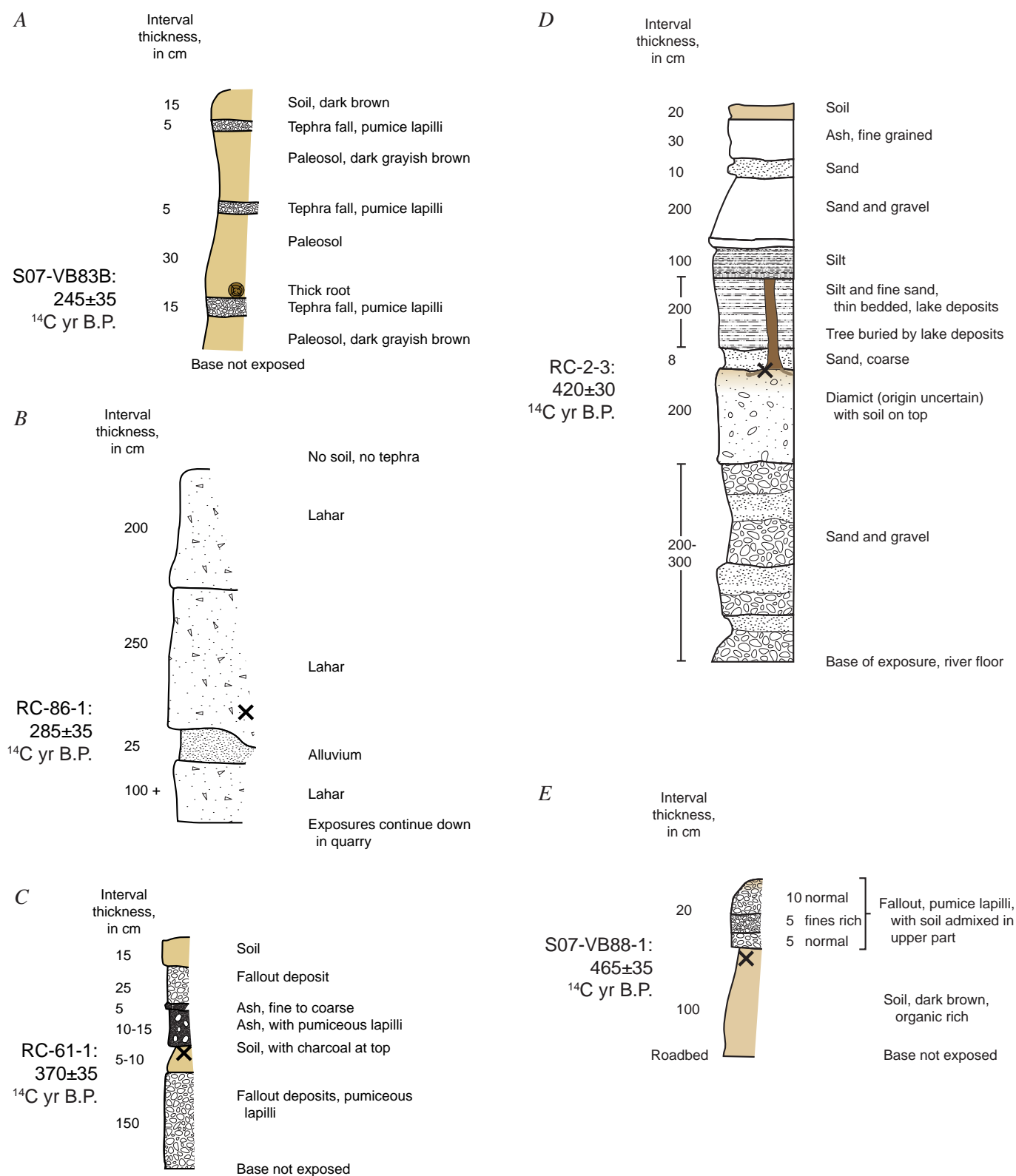
<sup>2</sup> Sample is root(?) collected 75 cm below ground surface near base of third paleosol downsection.

<sup>3</sup> Sample is from lahar deposit.

<sup>4</sup> Sample with Lab prefix I was reported by Linares and others (1975).

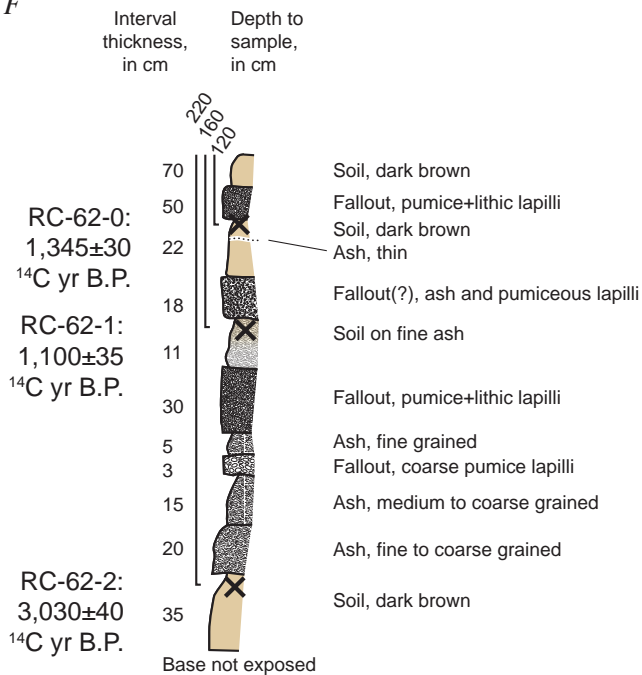
<sup>5</sup> Sample with Lab prefix Beta was collected and analyzed by Hermann Behling, from near the base of a 130-cm-deep core at Laguna Volcán (Behling, 2000).

**Figure 18.** Stratigraphic setting of radiocarbon samples collected January–February 2007 at Volcán Barú, Republic of Panamá. *A*, S07-VB83B; *B*, RC-86-1; *C*, RC-61-1; *D*, RC-2-3; *E*, S07-VB88-1; *F*, RC-62-0, RC-62-1, and RC-62-2; *G*, S07-VB56A; *H*, S07-VB98-2 and S07-VB98-1.

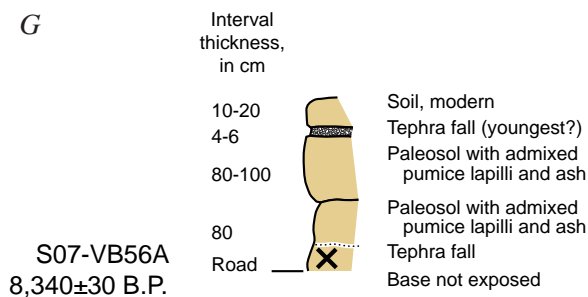




F



G



H

